

# ULTRA WIDEBAND TAPERED POWER COMBINER/DIVIDER

A THESIS

SUBMITTED TO THE DEPARTMENT OF ELECTRICAL AND  
ELECTRONICS ENGINEERING

AND THE GRADUATE SCHOOL OF ENGINEERING AND SCIENCE  
OF BILKENT UNIVERSITY

IN PARTIAL FULFILLMENT OF THE REQUIREMENTS

FOR THE DEGREE OF

MASTER OF SCIENCE

By

Okan Ünü

October, 2014

I certify that I have read this thesis and that in my opinion it is fully adequate, in scope and in quality, as a thesis for the degree of Master of Science.

---

Prof. Dr. Abdullah Atalar(Advisor)

I certify that I have read this thesis and that in my opinion it is fully adequate, in scope and in quality, as a thesis for the degree of Master of Science.

---

Assoc. Prof. Dr. Vakur Behçet Ertürk

I certify that I have read this thesis and that in my opinion it is fully adequate, in scope and in quality, as a thesis for the degree of Master of Science.

---

Assist. Prof. Dr. Aykutlu Dana

Approved for the Graduate School of Engineering and Science:

---

Prof. Dr. Levent Onural  
Director of the Graduate School

# ABSTRACT

## ULTRA WIDEBAND TAPERED POWER COMBINER/DIVIDER

Okan Ünlü

M.S. in Electrical and Electronics Engineering

Supervisor: Prof. Dr. Abdullah Atalar

October, 2014

Many typologies like the designs of Wilkinson Power Divider and Gysel Power Divider have been worked and improved through the years. Each design targets a higher bandwidth, a better isolation and a higher power handling capacity or smaller size. The basic analysis of every structure begins with the even mode and the odd mode models. The tapered lines are ultra wideband matching structures that are used to match real impedances. The only limitation of tapered line is the size, which has to be the half wavelength of the lower frequency limit. The tapered lines do not have any upper frequency cut-off. Because of the limitations in sizes, tapered lines have not been able to be used very commonly. The proposed new topology has a new taper topology with a single capacitor at the input side to decrease the lower frequency limit of the tapered line. The even mode structure of the proposed power divider/combiner is constructed of these improved tapered lines. In the odd mode analysis, the N section Wilkinson power divider/combiner design has been used. In order to determine the isolation resistor values, four different methods have been proposed. The proposed structure uses the surface resistive materials to implement these resistors. It has been observed that continuity of the isolation resistors between transmission lines causes some loss in the even mode. In order to solve this problem, the width of the resistors should be as small as possible to prevent the even mode loss.

*Keywords:* Microwave Power Combiner/Divider, Tapered Line, Wilkinson Power Divider, Microstrip Line.

## ÖZET

# ULTRA GENİŞ BANTLI GÜÇ BÖLÜCÜ BİRLEŞTİRİCİ

Okan Ünlü

Elektrik ve Elektronik Mühendisliği, Yüksek Lisans

Tez Yöneticisi: Prof. Dr. Abdullah Atalar

Ekim, 2014

Yıllar boyunca Wilkinson ve Gysel güç bölücü/birleştirici gibi bir çok topoloji üstünde çalışılmıştır. Her tasarım kendince daha geniş bantı, daha iyi izolasyonu, daha yüksek güç kapasitesini ve daha küçük boyutu hedeflemiştir. Her tasarım analizi basitleştirmek ve geliştirmek amacıyla, eşit durum ve ters durum analizleriyle ve basit eşleme elemanlarıyla başlar. Eğimli hatlı eşlemeler ultra geniş bantlı ve gerçek empedansları eşlemek için kullanılan basit yapılardır. Bu eşleme elemanları kendine has olarak frekans üst limitleri bulunmamaktadır ve tek limitleri boyutun en düşük frekans limitinin dalga boyunun yarısı ile sınırlı olmasıdır. Boyutlardaki limit nedeniyle bu yapılar çok sık kullanılmazlar. Eğimli hatları güç bölücü topolojilerinde kullanan eski tasarımlar mevcuttur. Önerilen tasarım eşit durumu analizinde tek bir kondansatör ile frekans alt limiti iyileştirilmiş bir eğimli hat kullanır. Ters durum analizi güç bölücü birleştirici tasarımındaki en gizemli kısımdır. Önerilen tasarımdaki ters durum analizi N bölümlü Wilkinson bölücü tasarımına benzemektedir ve izolasyon dirençlerinin seçimi için yeni empirik yöntemler öne sürülmüştür.

*Anahtar sözcükler:* Ultra geniş bantlı güç bölücü birleştirici, incelen iletim hattı, Wilkinson Güç birleştirici bölücü, micro şerit hat.

## Acknowledgement

”Confront them with annihilation, and they will then survive; plunge them into a deadly situation, and they will then live. When people fall into danger, they are then able to strive for victory.”

Sun Tzu

# Contents

- 1 Introduction 1**
  - 1.1 General Introduction . . . . . 1
  - 1.2 Examples of the generic power dividers/combiners . . . . . 3
  - 1.3 Tapered lines as wideband matching elements . . . . . 7
  - 1.4 Examples of power divider/combiner topologies with tapered lines 11
  
- 2 Analysis of Tapered Lines 13**
  - 2.1 Analytic tapered line design . . . . . 13
  - 2.2 Schematic implementation of tapered lines . . . . . 16
  - 2.3 EM simulation environment implementation of tapered line . . . . . 19
  - 2.4 Quarter wavelength size tapered line . . . . . 20
  
- 3 Analysis of Isolation Resistors 24**
  - 3.1 Equal power dissipation in isolation resistors . . . . . 24
  - 3.2 Linear variation for the isolation resistors . . . . . 30
  - 3.3 Bandwidth improvement of the isolation . . . . . 32

- 3.4 Power handling capacity of the proposed methods . . . . . 38
  
- 4 A Quarter Wavelength Tapered Power Divider/Combiner 43**

  - 4.1 Tapered power divider/combiner design . . . . . 43
  - 4.2 EM model of the new power divider/combiner design . . . . . 46
  - 4.3 Implementation of tapered power divider/combiner with discrete isolation resistors . . . . . 49
  - 4.4 EM model of the continuous isolation resistor power divider/combiner . . . . . 51

  
- 5 Conclusion 55**
  
- A Code 60**

# List of Figures

1.1	Standard 2-way Wilkinson divider topology. . . . .	3
1.2	Two way Wilkinson divider even mode analysis . . . . .	4
1.3	Two way Wilkinson divider odd mode analysis. . . . .	5
1.4	J. C. Kao 2-way divider/combiner topology. . . . .	6
1.5	A. Wentzel's modified topology for two stage Wilkinson. . . . .	7
1.6	Gysel Divider/Combiner topology . . . . .	8
1.7	The continuous tapered line(top) and the simplified tapered line (bottom) . . . . .	9
1.8	The tapered lines compared over reflection. . . . .	10
2.1	100 $\Omega$ to 50 $\Omega$ the exponential tapered line impedance change along $\bar{L}$	14
2.2	Microstrip line structure with the electric fields (left) and equiva- lent Microstrip Structure with the effective dielectric constant $\epsilon_r$ (right). . . . .	15
2.3	Tapered line model with discrete eight microstrip transmission line	17
2.4	The exponential tapered line schematic simulation with eight mi- crostrip transmission lines . . . . .	17



2.5	Embedded tapered line model of AWR software. . . . .	18
2.6	Embedded tapered line model simulation results. . . . .	18
2.7	The width of the tapered line change over normalized length with quadratic curve fitting. . . . .	19
2.8	Tapered line structure in the CST Microwave Studio . . . . .	20
2.9	S-parameters of exponential tapered line that is simulated with CST Microwave Studio from 1 to 10 GHz. . . . .	21
2.10	S-parameter simulation of the exponential tapered line from 0.5 to 4 GHz. . . . .	22
2.11	Smith Chart response of the S-parameter simulation of the exponential tapered line from 0.5 to 4 GHz. . . . .	22
2.12	New tapered line topology with the size of the quarter wavelength of minimum frequency. . . . .	23
2.13	Simulation result of the new tapered line from 0.5 GHz to 4 GHz. . . . .	23
3.1	The odd mode model of the power divider/combiner with the isolation resistors . . . . .	25
3.2	First two sections of the $N$ section power divider in the odd mode. . . . .	26
3.3	The odd mode schematic of the $N = 8$ section power divider/combiner . . . . .	28
3.4	The reflection of the $N$ section divider with equally power dissipating resistors in the odd mode . . . . .	30
3.5	The reflection of the $N$ section dividers with the linear decision option in the odd mode . . . . .	31

3.6	The reflection of the $N$ section divider with the improved equal power dissipation option in the odd mode . . . . .	33
3.7	The reflection of the $N$ section divider with the improved linear variation option in the odd mode . . . . .	34
3.8	Schematic model of odd mode where resistors have been replaced with ports. . . . .	38
3.9	Power dissipation results of the resistors for the linear variation method . . . . .	39
3.10	Power dissipation results of the resistors for the equal power dissipation option . . . . .	39
3.11	Power dissipation results of the resistors for the bandwidth improved equal power dissipation option . . . . .	40
3.12	Power dissipation results of the resistors for the bandwidth improved linear resistor decision option . . . . .	40
3.13	Power dissipation results of the resistors for the optimized Wilkinson resistors . . . . .	41
4.1	Schematic model of the new tapered power divider/combiner design.	44
4.2	S-parameter simulation results of the new power divider design . .	44
4.3	Schematic model of eight section Wilkinson power combiner divider design. . . . .	45
4.4	S-parameter simulation results of the eight section Wilkinson power divider design . . . . .	45
4.5	The designed combiner/designer with the discrete resistors. . . . .	47

4.6	EM structure of the designed combiner/designer with the discrete resistors. . . . .	48
4.7	EM Simulation of designed power combiner/designer with extended bandwidth. . . . .	48
4.8	Realization of discrete resistor design . . . . .	50
4.9	Network Analyzer Results of realized design with discrete resistors	50
4.10	EM Model of continuous isolation resistance. . . . .	51
4.11	EM Simulation of continuous tapered divider with $50 \Omega/\text{sq}$ surface resistive material . . . . .	52
4.12	Visualization of even mode loss, red resistors are models of continuous resistor, blue waves are signals and green line is the connection between peaks of the signals. . . . .	53
4.13	EM Simulation of continuous tapered divider with $1000 \Omega/\text{sq}$ surface resistive material . . . . .	54
5.1	Design guideline for the proposed power divider combiner. . . . .	57

# List of Tables

2.1	The exponential tapered line impedance and corresponding width on microstrip . . . . .	16
3.1	The isolation resistors and the intermediate impedances for the $N = 8$ section divider in the odd mode . . . . .	28
3.2	Equally power dissipating resistor values and the bandwidth for the $N$ section power divider . . . . .	30
3.3	The resistor values decided with linear variation and the bandwidths for the different $N$ section power dividers . . . . .	31
3.4	Bandwidth comparisons of different resistor decision methods with different $N$ . . . . .	35
3.5	Figure of merit and $\bar{L}$ results of different resistor decision methods	37
3.6	$\gamma$ values of the different resistor decision methods with different $N$	42

# Chapter 1

## Introduction

### 1.1 General Introduction

This thesis introduces a new type of ultra wideband (UWB) power divider/combiner with tapered lines and N section isolation resistors. The tapered lines are matching structures without a theoretical upper frequency limit. The tapered lines are limited to a lower cutoff frequency (which is  $\lambda/2$  of tapered line). The lower frequency has been reduced to the  $\lambda/4$  frequency by adding a series capacitance to the input port. Consequently, we achieve a power divider about the same size with the classical Wilkinson power divider with an ultra high bandwidth.

A desired power divider/combiner is a three port device, in which all ports are assumed to be terminated in  $Z_0$  impedance. The power that is going into port 1 is divided equally between ports 2 and 3 (divider). Similarly, the power going into the port 2 and the port 3 (that have the same phases) is added on the port 1 (combiner)[1].

The basic network theory proves that it is impossible to achieve a three-port network, which is reciprocal, lossless and matched at the same time. A very simple power divider/combiner can be achieved with a T-junction that is reciprocal and lossless, but not matched. Even when it is acceptable to use an unmatched three

port, the isolation is still a problem. The isolation is important for the systems with redundancy and failure tolerance requirements. It is also possible to use the lossy resistive dividers where the power efficiency is not critical. The power is divided with the same ratio; however, a significant amount of the power is lost on some elements in the system.

Aside from reciprocity, loss and matching of the power divider, there are other requirements such as frequency, bandwidth, split ratio, power handling capacity, etc. These requirements are application specific, but affect the design directly. Frequency and bandwidth are directly related to the topology size. Due to its nature, when a power divider needs to achieve a wide bandwidth, the design requires distributed elements that can work at low frequencies; thus, the size of the topology directly increases. Additionally, the power handling capacity decreases due to the smaller size of each element (i.e, smaller resistors, capacitors and transmission lines) as the frequency increases.

The bandwidth and size in terms of wavelength comparison has been made among different types of power dividers. The bandwidth ( $BW$ ) is defined as a ratio of upper frequency ( $f_2$ ) and lower frequency ( $f_1$ ) limits:

$$BW = f_2/f_1 \tag{1.1}$$

The total size of the structure is also normalized with the wavelength at the lowest frequency  $\lambda_1$  such as:

$$\bar{L} = L/\lambda_1 \tag{1.2}$$

$\bar{L}$  is a variable that represents the total length compared to the lowest frequency wavelength. For example, if the total size of a topology is a quarter wavelength at  $f_1$ , then  $\bar{L} = 1/4$ . The figure of merit ( $FoM$ ) for  $N$  section power dividers is defined as:

$$FoM = BW/\bar{L} \tag{1.3}$$

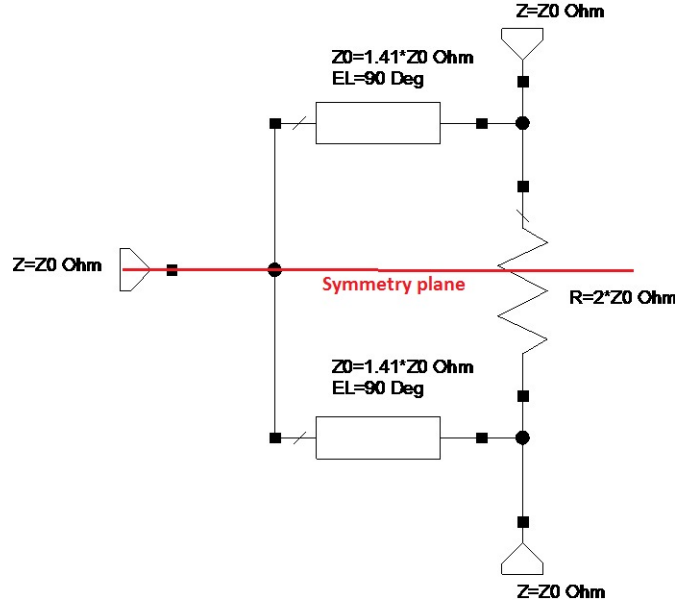


Figure 1.1: Standard 2-way Wilkinson divider topology.

## 1.2 Examples of the generic power dividers/-combiners

The Wilkinson power divider/combiner is a narrow band structure [2]. In order to reduce the problem, our discussion will be continued with a 2-way Wilkinson power divider. A 2-way Wilkinson power divider consists of two  $\lambda/4$  section transmission lines, which have  $\sqrt{2}Z_0$  line impedance, in which all of the ports are terminated with  $Z_0$  impedances. Furthermore, there is a resistor which has a  $2Z_0$  resistance between the port 2 and the port 3. The discussion of the Wilkinson divider is trivial, however, the basic analysis is very important due to its very common use in this thesis.

The analyses of the divider begin with **the even mode** and **the odd mode** analyses. For both of the analyses, it is assumed that the signals are induced from port 2 and port 3. Therefore, there is a symmetry plane just in the middle of the structure (Fig. 1.1). The even mode analysis assumes that signals induced from port 2 and port 3 have the same phase and the same magnitude. While both of the signals have the same phase and the same magnitude, the symmetry

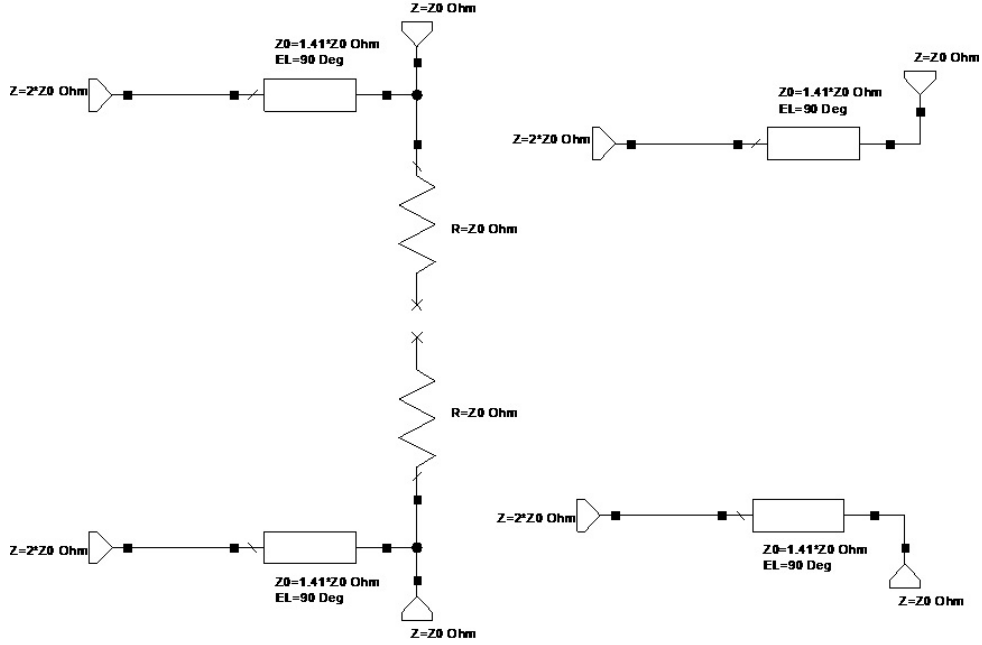


Figure 1.2: Two way Wilkinson divider even mode analysis

works like an open circuit. Therefore, the circuit can be simplified as given in Figure 1.2. While the symmetry plane is an open circuit, the resistor is divided in half and it is connected to an open circuit. Thus, the resistors do not have any effect on the even mode. The input port is just on the symmetry plane, and it is also separated from the other half of the circuit. Hence, the impedance of port 1 is doubled due to the parallelism with its mirror. It can be easily observed that the  $\lambda/4$  transmission line is just a quarter wave transformer that matches  $Z_0$  to  $2Z_0$ . The quarter wave transformer equation shows that:  $Z_{in} = Z_{line}^2 / Z_L$  where  $Z_L = Z_0$  and  $Z_{in} = 2Z_0$ . This gives the characteristic impedance of the transmission line as,  $Z_{line} = \sqrt{2}Z_0$  [1].

The signals coming from the port 2 and the port 3 have the opposite phase in the odd mode analysis. Therefore, the symmetry plane becomes a short circuit in the odd mode. The resistor is halved again, but this time it is grounded. Interestingly, port 1 is also directly grounded in the odd mode, thus there is not any concern with the port 1 (Fig. 1.3). Basic network analysis shows that while the transmission line is a quarter wavelength, the short circuit (or ground) is transformed to an open circuit. The half of the resistor is already  $Z_0$ , therefore



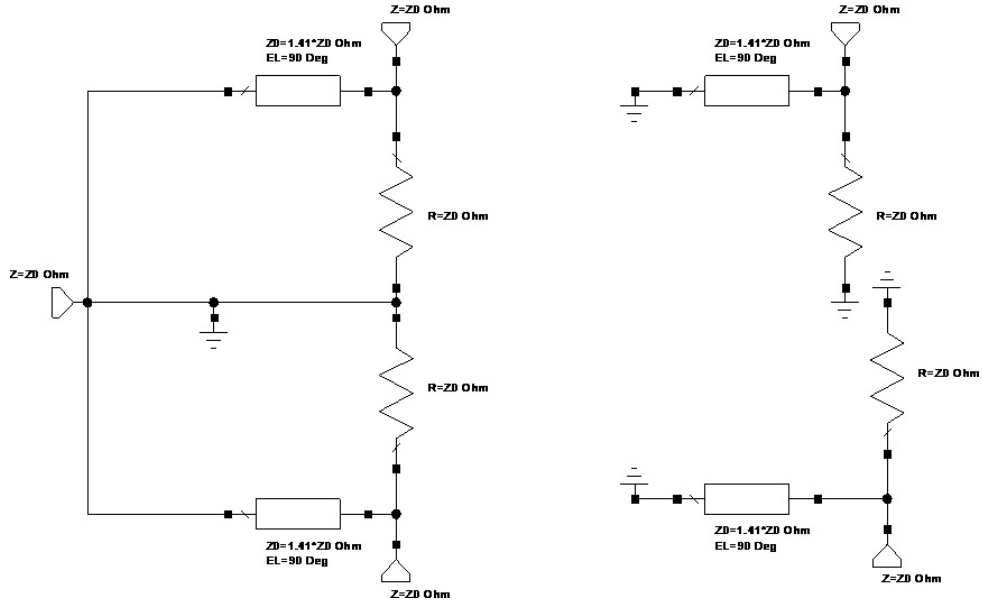


Figure 1.3: Two way Wilkinson divider odd mode analysis.

the port is matched[1].

The analysis shows that the impedance of port 1 depends on the even mode structure. Similarly, the odd mode analysis gives the isolation resistor's value. The isolation level depends on the odd mode topology. If matching of port 1 is appropriate on the even mode analysis, the overall matching of the port 1 of the power divider/combiner is appropriate. If the other ports are matched in the odd mode, then the isolation level is also appropriate. It is not possible to say the same thing for the impedances of port 2 and port 3. Impedances of the port 2 and 3 are both affected from the even mode and the odd mode.

A multistage Wilkinson power divider/combiner is a common solution for the wideband applications. The multistage Wilkinson power divider/combiner has a large size depending on the number of sections. Besides, there is not any simple approach to the calculations of transmission lines, the number of stages required and the values of isolation resistors for a given bandwidth. There are tables for giving the number of sections and the required bandwidth given by Cohn [3].

There are many other designs similar to Wilkinson's design, which are targeting to achieve a higher bandwidth with additional components. J.C. Kaos

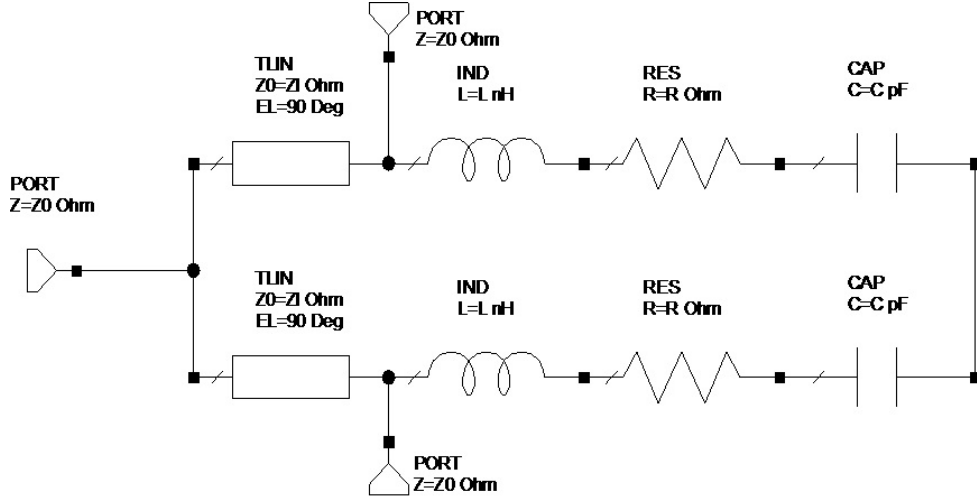


Figure 1.4: J. C. Kao 2-way divider/combiner topology.

design is a good and a new example of additional components [4]. The topology uses Wilkinson power divider as a base and adds lumped elements to the isolated network. (Fig. 1.4) Therefore, the additional network increases only the isolation bandwidth.

A similar approach can be found in Ou and Chu's work [5]. In this design matching elements are used in the even mode and the odd mode. The structure is similar to the two stage Wilkinson with an addition of an open stub matching to the middle stage. The achieved bandwidth may be satisfactory, but the matching condition is assumed to be -10 dB for both isolation and reflection. There is also a very similar topology from O. Ahmed with one less component. They have the same matching and isolation condition levels in their works [6].

The other two modified Wilkinson topologies can be found in A. Wentzel's paper [7]. Both of the topologies add some lumped components to the network. Those structures are also increasing the bandwidth, but the condition for the matching is -12 dB in the frequency band. (Fig. 1.5)

Aside from the Wilkinson dividers, there are also other combiner types such as the Gysel power divider/combiner [8], which has a narrower bandwidth compared to the Wilkinson divider, yet still an accepted and used power divider/combiner topology due to its high power handling capacity. The isolation resistors of the

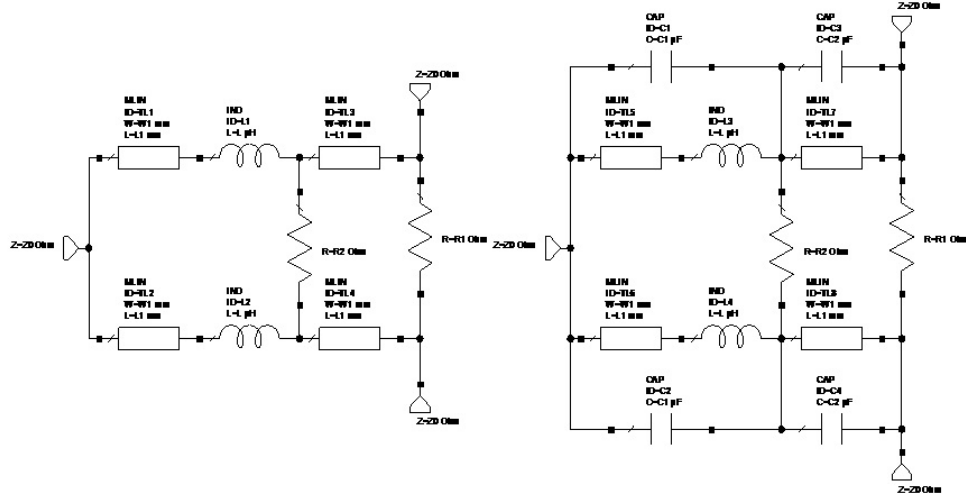


Figure 1.5: A. Wentzel's modified topology for two stage Wilkinson.

Gysel divider/combiners are connected to separate ports. Thus, the resistors can be connected to the ground. Since the ground is a good heat sink, the power is easily dissipated.

### 1.3 Tapered lines as wideband matching elements

In the literature, it can be observed that nearly all of the different types of divider/combiner topologies use different matching structures for a better impedance matching, a good pass band and a high isolation. The problem can be simplified to a matching problem for the even mode analysis. In this context, the tapered lines are very good examples of ultra wideband matching of real impedances.

A tapered line is a finite transmission line whose characteristic impedance changes continuously over its length. The common analytic approach is to simplify the tapered line as a  $N$ -section transmission line, where every section has a length of  $\Delta x$ . Thus, the total length of the tapered line becomes  $L = N\Delta x$ . The impedance of tapered line changes from  $Z_{in}$  to  $Z_{out}$  continuously as a function of

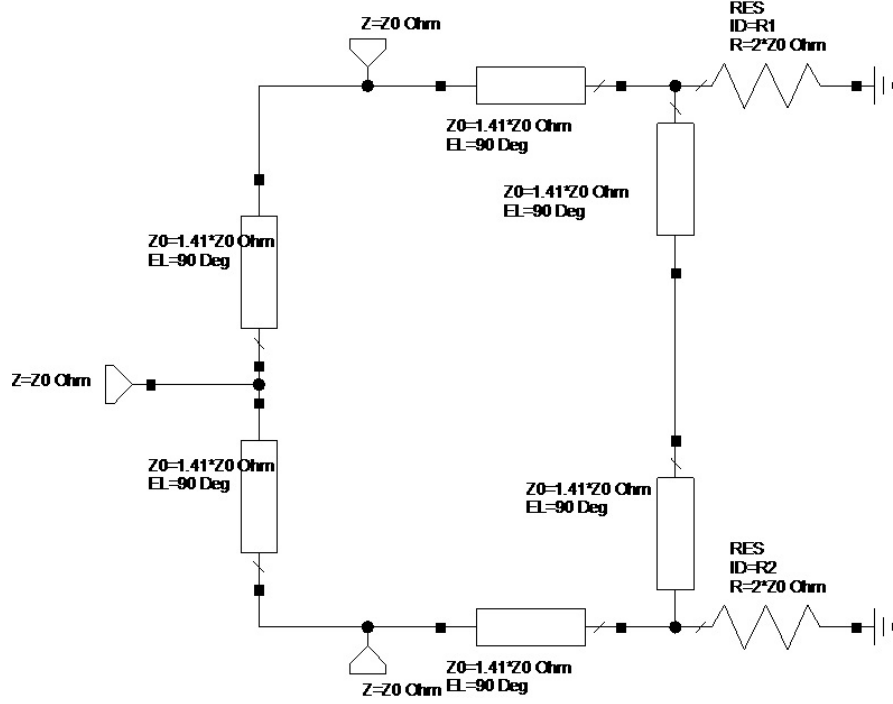


Figure 1.6: Gysel Divider/Combiner topology

$x$  so that  $Z(0) = Z_{in}$  and  $Z(L) = Z_{out}$ . The problem is to minimize the reflection for a function of  $Z(x)$  [9] [1].

In order to find a proper  $Z(x)$ , it is crucial to find the total reflection caused by each reflection along the tapered line. The partial reflection can be defined as:

$$\Delta\Gamma = \frac{(Z + \Delta Z) - Z}{(Z + \Delta Z) + Z} \cong \frac{\Delta Z}{2Z} \quad (1.4)$$

where  $\Delta Z$  is the impedance change and  $\Delta\Gamma$  is the reflection due to the impedance change for a section of  $\Delta x$  at the position of  $x$ . The exact differential becomes

$$d\Gamma = \frac{dZ}{2Z} = \frac{1}{2} \frac{d(\ln Z/Z_{in})}{dx} dx \quad (1.5)$$

By using the small reflection theory, the total reflection at the input port can be written as

$$\Gamma(\theta) = \frac{1}{2} \int_{x=0}^L e^{-2j\beta z} \frac{d}{dx} \ln \left( \frac{Z(x)}{Z_{in}} \right) dx \quad (1.6)$$

If  $Z(x)$  is known, it is straightforward to find the reflection, although the inverse of the function is quite challenging to solve. There are several known and used

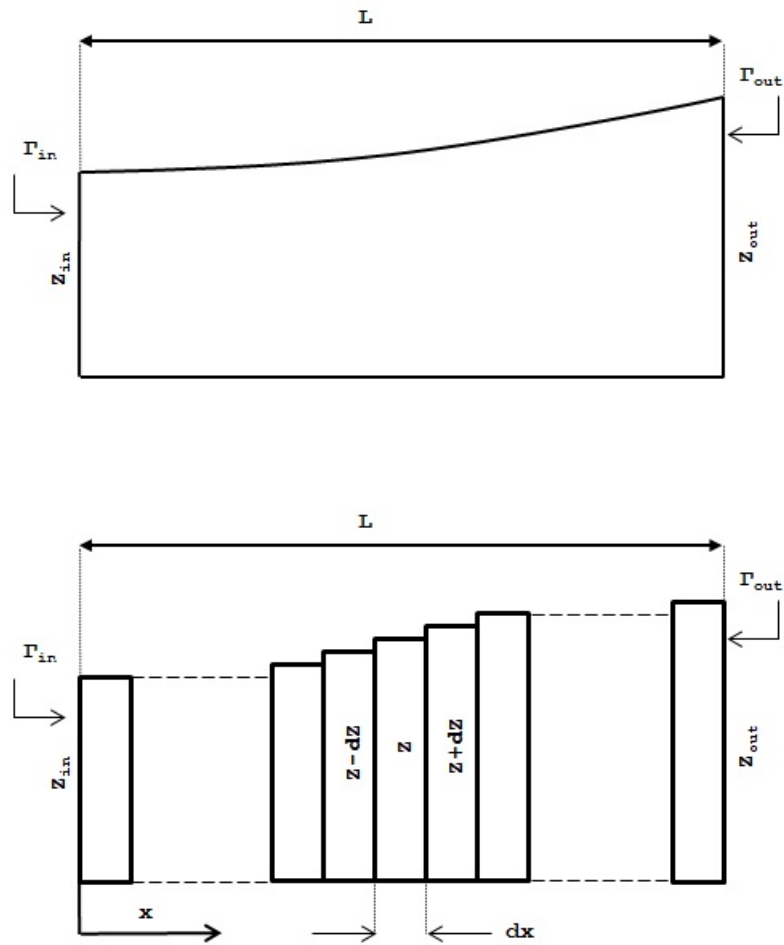


Figure 1.7: The continuous tapered line(top) and the simplified tapered line (bottom)

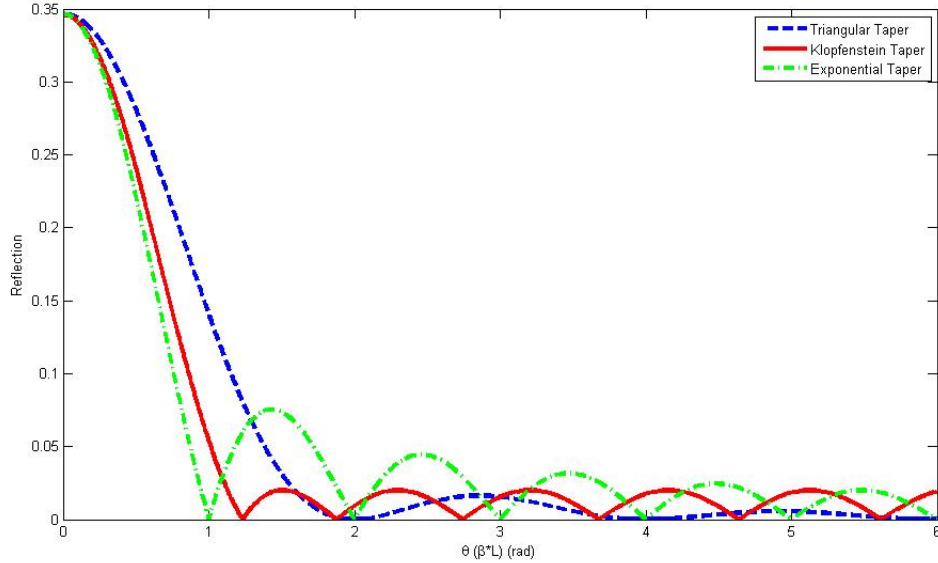


Figure 1.8: The tapered lines compared over reflection.

functions for  $Z(x)$  and these functions are the exponential taper, the triangular taper and the Klopfenstein taper.

The exponential taper is probably the most common taper type which has a very simple formula:

$$\begin{aligned} Z(x) &= Z_{in}e^{ax} & (1.7) \\ a &= \frac{1}{L} \ln \left( \frac{Z_{out}}{Z_{in}} \right) \end{aligned}$$

where  $L$  is the total length of the taper. The reflection from this type of taper is formulated as:

$$\Gamma = \frac{\ln Z_{out}/Z_{in}}{2} e^{-j\beta L} \frac{\sin \beta L}{\beta L} \quad (1.8)$$

The Klopfenstein taper is also a very popular taper type that gives the optimum reflection response over the passband [10]. The Klopfenstein taper uses the Chebyshev functions and has a very complex line impedance formula for given  $Z_{in}$  and  $Z_{out}$ . Similarly, a triangular taper gives an appropriate response over the pass band.

Theoretically, the only limitation of the tapered line is the lower cutoff frequency. The minimum frequency cutoff is the half wavelength equivalent

( $\bar{L} = 1/2$ ) for the exponential taper. The pass band starts slightly higher than the half wavelength for the Klopfenstein taper ( $\bar{L} \geq 1/2$ ). Whereas, the pass band starts from the full wavelength ( $\bar{L} = 1$ ) for the triangular taper (Fig. 1.8).

## 1.4 Examples of power divider/combiner topologies with tapered lines

The power divider/combiner topologies with the tapered lines exist in the literature. P.C. Goodman's stripline combiner/divider design is the first example [11]. The topology simply consists of two tapered lines instead of the quarter wave transformers and a continuous isolation resistor between them. Goodman achieves good results on matching and isolation; however, he has not been able to define any type of equation for the isolation resistance. He has experimentally found a proper shape and surface resistance. He has also stated that the shape of the resistance between lines causes an undesirable loss in the even mode.

F.C de Ronde's design is very similar to Goodman's as he has successfully achieved a multi-octave divider/combiner design [12]. The design is based on a slotted circular taper and a resistive layer between them. He has also added two open stub matching components to the input side of the lower frequency limit. Even if he has stated that there are functions for the resistors and the sizes in the design, he has not provided those functions in the paper. One of the most important points is that, he has achieved a quarter wave size design ( $\bar{L} = 1/4$ ). The design overall looks like an experimental result similar to Goodman's. Ronde has compared his design to the multistage Wilkinson and has found out that his design has a smaller structure. The problem with his design is that he has not stated any analytic reasoning.

The newest design in B. Menca-Oliva's paper is very close to the approach of this thesis[13]. The paper gives a complete solution and a design approach for a wide band tapered power divider/combiner design. The approach can be explained in two steps. It begins with a tapered line design that is a Klopfenstein

taper. Those tapers are used in the even mode. The proper discrete resistors and the positions of the resistors are found experimentally for the desired bandwidth. The structure has very efficient results in terms of bandwidth. On the other hand, the design is still a half wavelength size ( $\bar{L} = 1/2$ ) and the maximum frequency of isolation band is limited due to the use of discrete components.



# Chapter 2

## Analysis of Tapered Lines

### 2.1 Analytic tapered line design

This section is about the even mode analysis for the proposed structure. In this chapter, the main objective is to define a structure that contains a tapered line with a quarter wavelength that matches the even mode ports. In order to simplify the structure, the ports are assumed to be terminated in  $50 \Omega$ . The target frequency band will start from 1 GHz and the upper frequency limit of the divider combiner design will be decided in the odd mode analysis.

The proposed structure will be a microstrip structure on Rogers Duroid 4003C with 20 mil thick substrate. Therefore, the wavelength comparison will be made on this structure. The Rogers 4003C material's dielectric constant is  $\epsilon_r = 3.38$ . As discussed in the Chapter 1, the input termination is doubled,  $Z_{in} = 100\Omega$  and the output termination stays the same,  $Z_{out} = 50\Omega$  in the even mode. Even though there are better examples of the different tapered lines as discussed in Chapter 1, the exponential taper should be used due to its simplicity and slightly better frequency response. The exponential taper equation is given as:

$$Z(x) = Z_{in}e^{ax} \tag{2.1}$$
$$a = \frac{1}{L} \ln \left( \frac{Z_{out}}{Z_{in}} \right)$$

Where the impedances have been replaced with  $Z_{in} = 100\Omega$ ,  $Z_{out} = 50\Omega$ . Figure 2.1 demonstrates how the impedance changes from  $100\Omega$  to  $50\Omega$  along the exponential tapered line.

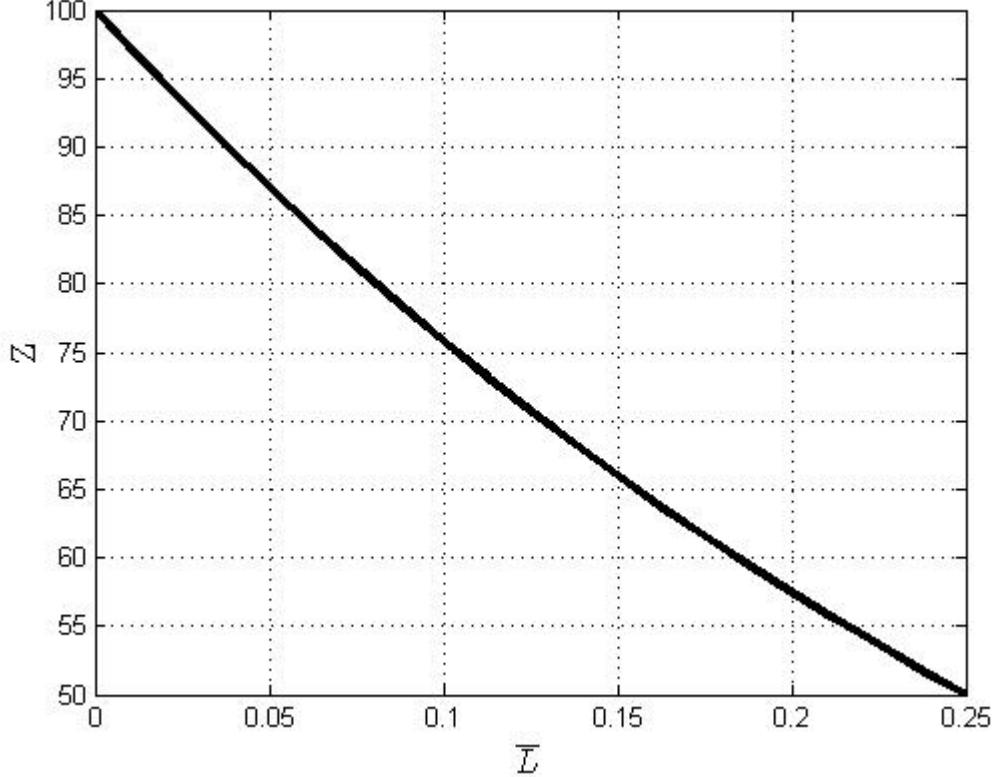


Figure 2.1:  $100\Omega$  to  $50\Omega$  the exponential tapered line impedance change along  $\bar{L}$

Since the main structure of the divider is microstrip line, for the given characteristic impedance  $Z$ , the dielectric constant  $\epsilon_r$ , and the substrate thickness  $t_{subs}$ , the width of the microstrip can be calculated as;

$$W = \begin{cases} \frac{8de^A}{e^{2A}-2} & \text{for } W < 2d \\ \frac{2d}{\pi} \left[ B - 1 - \ln(2B - 1) + \frac{\epsilon_r - 1}{2\epsilon_r} \left\{ \ln(B - 1) + 0.39 - \frac{0.61}{\epsilon_r} \right\} \right] & \text{for } W \geq 2d \end{cases} \quad (2.2)$$

where  $A$  and  $B$  are,

$$A = \frac{Z}{60} \sqrt{\frac{\epsilon_r + 1}{2}} + \frac{\epsilon_r - 1}{\epsilon_r + 1} + \left(0.23 + \frac{0.11}{\epsilon_r}\right)$$

$$B = \frac{377\pi}{2Z\sqrt{\epsilon_r}}$$

The width of the exponential tapered line can be calculated from 100  $\Omega$  to 50  $\Omega$  by using equation 2.2. Additionally, it is necessary to calculate the length of the structure. The frequency requirement for the lower cutoff is at 1 GHz and the structure needs to be a quarter wavelength of that frequency.

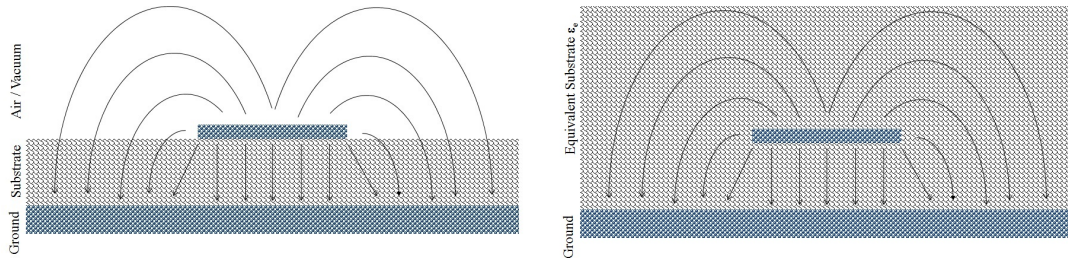


Figure 2.2: Microstrip line structure with the electric fields (left) and equivalent Microstrip Structure with the effective dielectric constant  $\epsilon_r$  (right).

It is not feasible to use the dielectric constant of the substrate directly for the microstrip line. The generic wavelength equation stays the same; however, it is necessary to use an effective dielectric constant for the calculations of the wavelength.

$$\lambda = \frac{f}{c\sqrt{\epsilon_e}} \quad (2.3)$$

Where  $\epsilon_e$  is defined as:

$$\epsilon_e = \frac{\epsilon_r + 1}{2} + \frac{\epsilon_r - 1}{2} \frac{1}{\sqrt{1 + 12d/W}} \quad (2.4)$$

The equation shows that effective dielectric constant is directly related to the width  $W$  of the microstrip. However, the tapered line structure's width changes over the length. If the line had only been 50  $\Omega$ , from the given equations 2.3 and 2.4,  $\epsilon_e = 2.78$  thus  $\lambda_{microstrip} = 180 \text{ mm}$  at 1 GHz. Similarly, if the line had only been 100  $\Omega$ , from the given equations  $\epsilon_e = 2.54$  thus  $\lambda_{microstrip} = 188 \text{ mm}$  at 1 GHz. For 70  $\Omega$ , which is Wilkinson divider's line impedance,  $\lambda_{microstrip} =$

Table 2.1: The exponential tapered line impedance and corresponding width on microstrip

$Z_{even}$ of the tapered line ( $\Omega$ )	$W$ of the tapered line (mm)
100.00	0.287
92.58	0.374
85.72	0.415
79.37	0.491
73.49	0.575
68.04	0.667
63.00	0.769
58.33	0.88
54.00	1.00
50.00	1.13

184 mm and it will be taken into account as the minimum frequency's wavelength which is  $\lambda_{max}$ . From the given calculations, the length of the structure becomes  $L = \lambda_{1GHz}/4 = 46$  mm.

## 2.2 Schematic implementation of tapered lines

Knowing the impedance of the exponential tapered lines and the total length, the simulator from AWR Corp. is used to make a schematic simulation. As explained in Chapter 1, the tapered lines can be approximated with  $N$  number of transmission lines. The characteristic impedance of any transmission line section  $n$  can be calculated as:

$$Z_{even}(n) = Z_{in}e^{an} \quad (2.5)$$

$$a = \frac{1}{N+1} \ln\left(\frac{Z_{out}}{Z_{in}}\right)$$

where  $n = 1, 2, \dots, N$  and the exponential taper equation 2.1 is approximated for any arbitrary  $N$  section. The tapered line is simplified as  $N = 8$  discrete transmission lines (Fig. 2.3). Every section of the transmission line will be  $L_d = 5.74$  mm. Thus, the total length of the tapered line will be  $L = 8L_d = 46$  mm. The widths of each section are given in Table 2.1.

Table 2.1 includes 50  $\Omega$  and 100  $\Omega$ . 100  $\Omega$  and 50  $\Omega$  widths and the transmission lines are not added to the circuit since they do not have any effect on the matching while the connected ports of these transmission lines are already 50  $\Omega$  and 100  $\Omega$ .

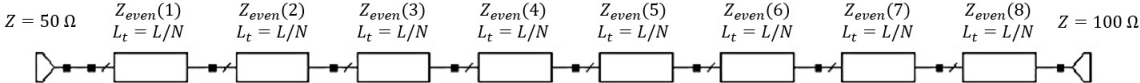


Figure 2.3: Tapered line model with discrete eight microstrip transmission line

The resulting S-parameters of the given structure are very close to the exponential tapered line response (Fig. 2.4). While  $\lambda_{1GHz}/4 = 46 \text{ mm}$  at 1 GHz, the response is not efficient as expected. On the other hand, near 2 GHz the reflection is far below -20 dB and it stays below -20 dB for the rest of the pass band. Since the tapered line is sampled for this example, there is an upper frequency limit which is approximately 15 GHz. If the number of the discrete sections is increased, a higher frequency limit is achievable. This upper frequency limitation will not appear in a continuous model of the tapered line.

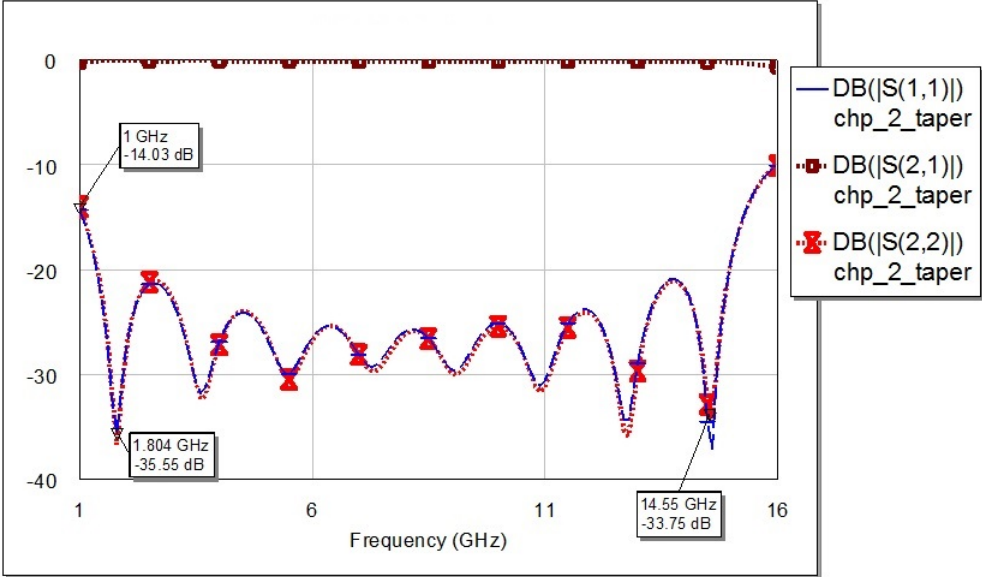


Figure 2.4: The exponential tapered line schematic simulation with eight microstrip transmission lines

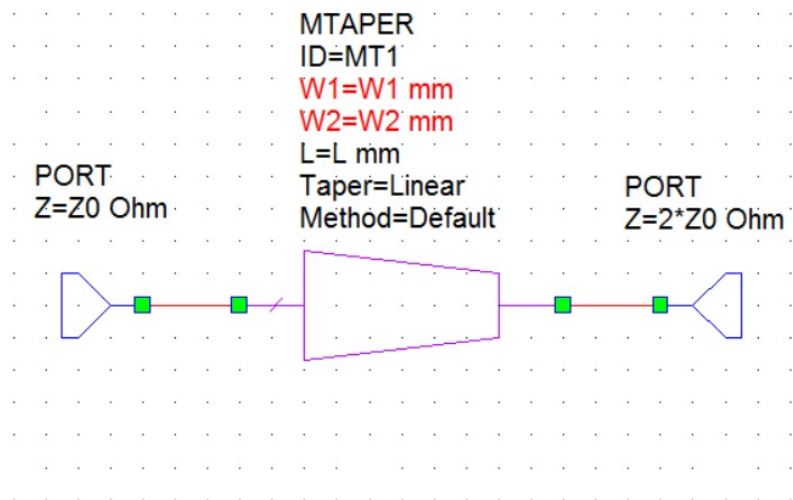


Figure 2.5: Embedded tapered line model of AWR software.

Even if it is shown that tapered line can be simulated with  $N$  sections of the transmission line, the simulator from AWR Corp. already contains a tapered line model. The tapered line model can be selected as the exponential (Fig. 2.5). The default methodology of this AWR element is exactly same as our model's. AWR software discretizes the tapered line into the smaller transmission line sections depending on the simulation frequency range. Therefore, the resulting simulation is very similar to the previous example with a larger bandwidth (Fig 2.6).

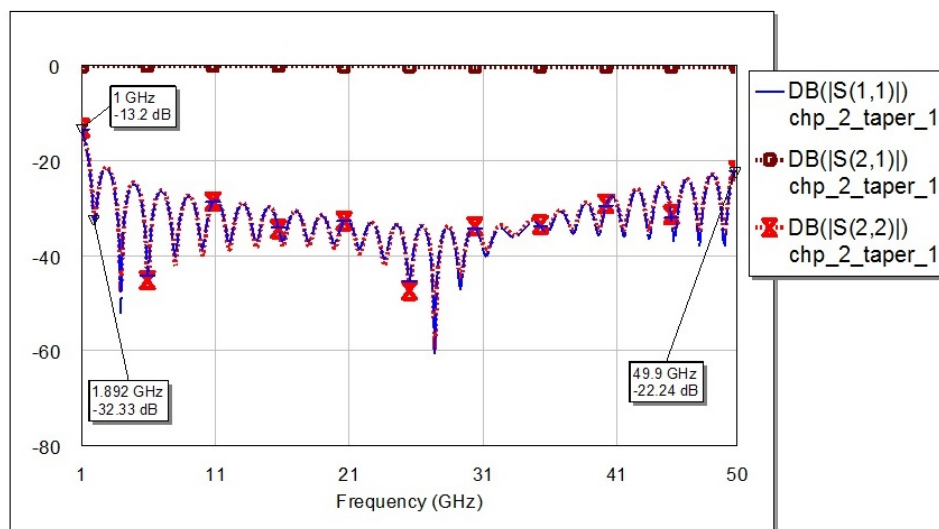


Figure 2.6: Embedded tapered line model simulation results.

## 2.3 EM simulation environment implementation of tapered line

The tapered line is a continuous structure, therefore it is necessary to simplify the model analytically in order to implement in EM model. CST Microwave Studio allows users to use analytic expressions for defining shapes. In order to find a proper equation, the MATLAB Curve Fitting Toolbox is used. The line is already similar to a 2nd order polynomial in which the entire constants are positive,

$$W(x) = p_1x^2 + p_2x + p_3 \quad (2.6)$$

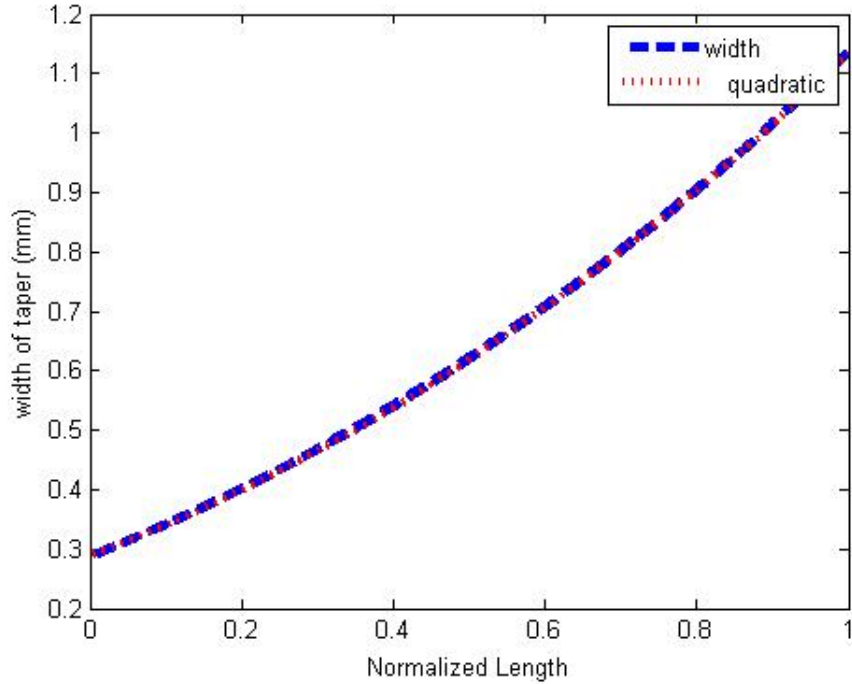


Figure 2.7: The width of the tapered line change over normalized length with quadratic curve fitting.

In order to simplify the model, Figure 2.7 is drawn with the x axis which is normalized to 1. Therefore, it can be extended to any given length. A quadratic curve fitting gives the coefficients of  $p_1 = 0.36547$ ,  $p_2 = 0.4767$  and  $p_3 = 0.29007$ . The equation that is used to model an analytic curve defines the borders of the tapers. The resulting structure is given in the Figure 2.8.

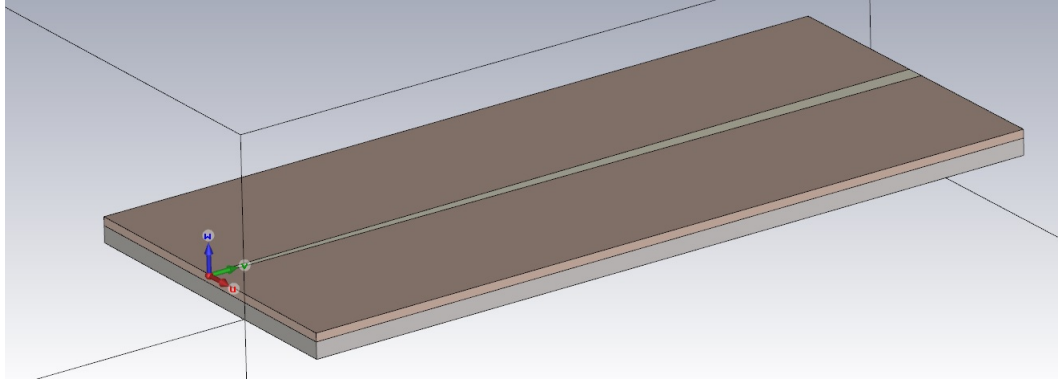


Figure 2.8: Tapered line structure in the CST Microwave Studio

The frequency bandwidth for the CST simulation has been chosen between 1 GHz to 10 GHz. Figure 2.9 displays the EM simulation results that are very close to what had been simulated in the schematic simulations.

## 2.4 Quarter wavelength size tapered line

Until this section it has been shown how an exponential taper line is designed. The important part of this section is that the new structure brings a competition to a Wilkinson power divider or to a quarter wave transformer. It is good to look at the Smith chart response of the standard tapered line.

It can be observed from the Smith chart that the lower frequency has some positive reactance from  $100 \Omega$  port side (Fig 2.11). Adding a series capacitance compensates the reactance for lower frequencies and does not affect the response of the higher frequencies due to the equation  $Z_c = 1/j\omega C$ .

A series capacitor has been added to the input of the previously designed tapered line and the value of the capacitor can be found by trial and error. (Fig. 2.12) For this example, it is 6pF. The new tapered line topology reduces the lower frequency limit down to 1 GHz for 20 dB return loss limit (Fig. 2.13). This capacitance value can be calculated numerically. The Smith chart shows that  $x = 0.38j$  should be matched. This value is normalized with  $Z_0 = 100\Omega$ . Thus,



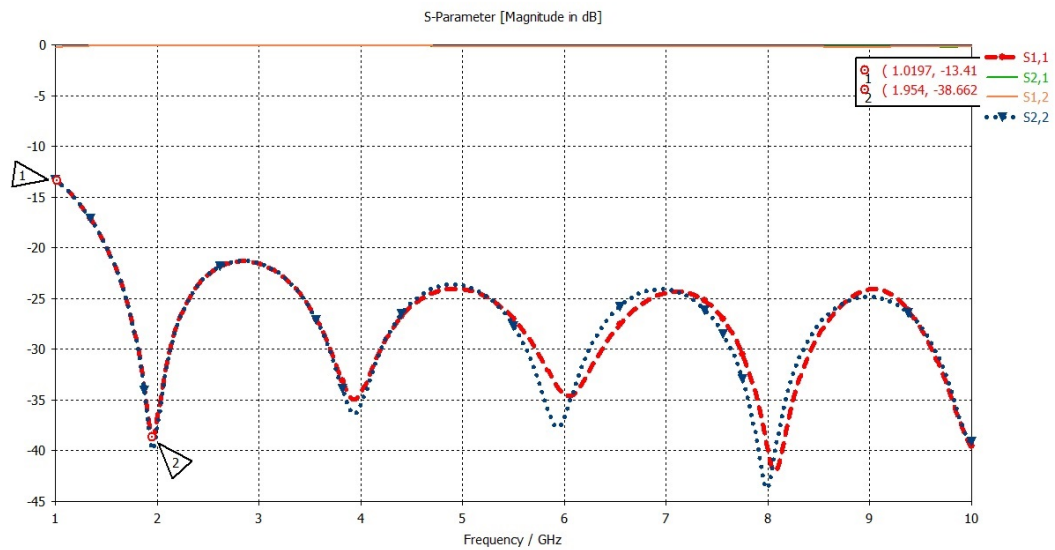


Figure 2.9: S-parameters of exponential tapered line that is simulated with CST Microwave Studio from 1 to 10 GHz.

imaginary part that should be matched is  $X = 38j\Omega$ . The proposed solution is adding a series capacitance  $Z_C = \frac{1}{j\omega C}$  and  $\omega = 2\pi f$  where  $f = 1GHz$ . If  $Z_C = -38j$  than  $C = 4.2$  pF, which is slightly below 6pF.

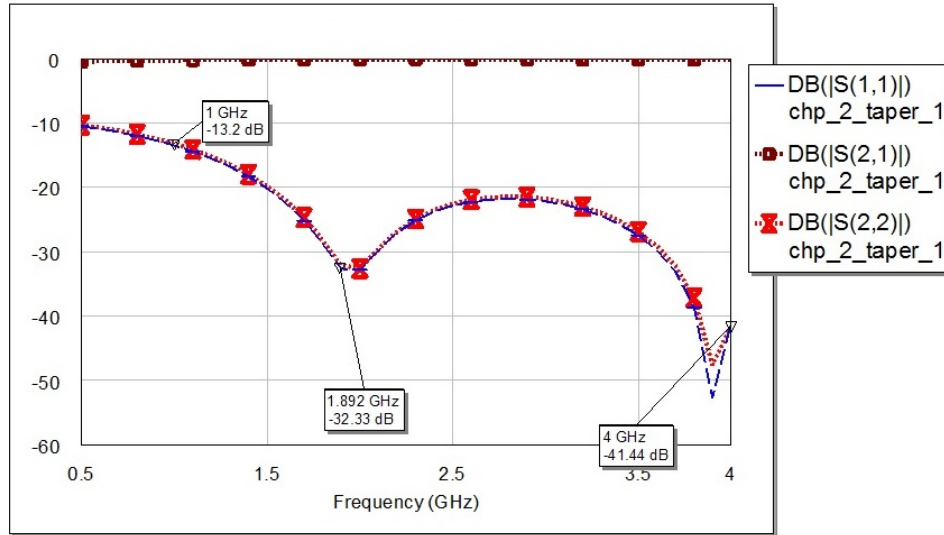


Figure 2.10: S-parameter simulation of the exponential tapered line from 0.5 to 4 GHz.

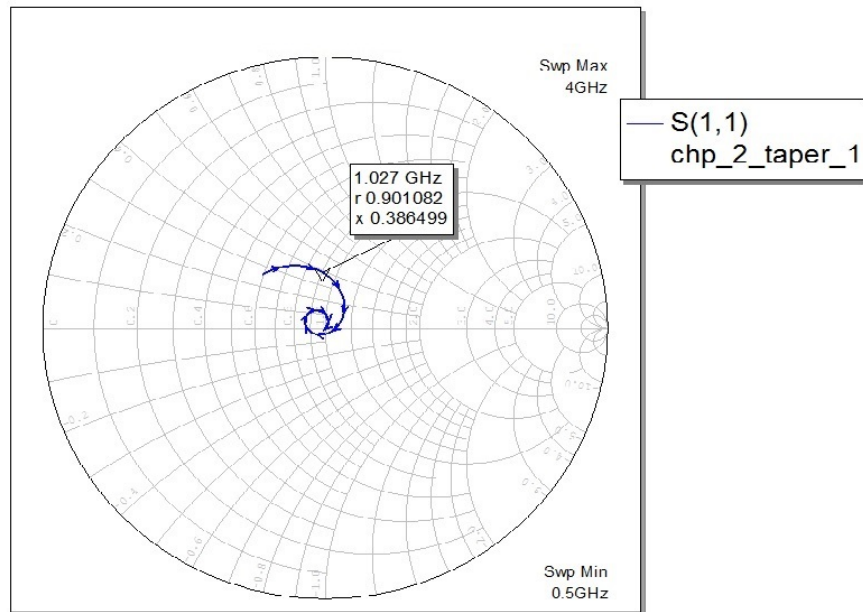


Figure 2.11: Smith Chart response of the S-parameter simulation of the exponential tapered line from 0.5 to 4 GHz.

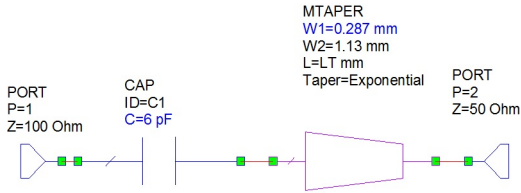


Figure 2.12: New tapered line topology with the size of the quarter wavelength of minimum frequency.

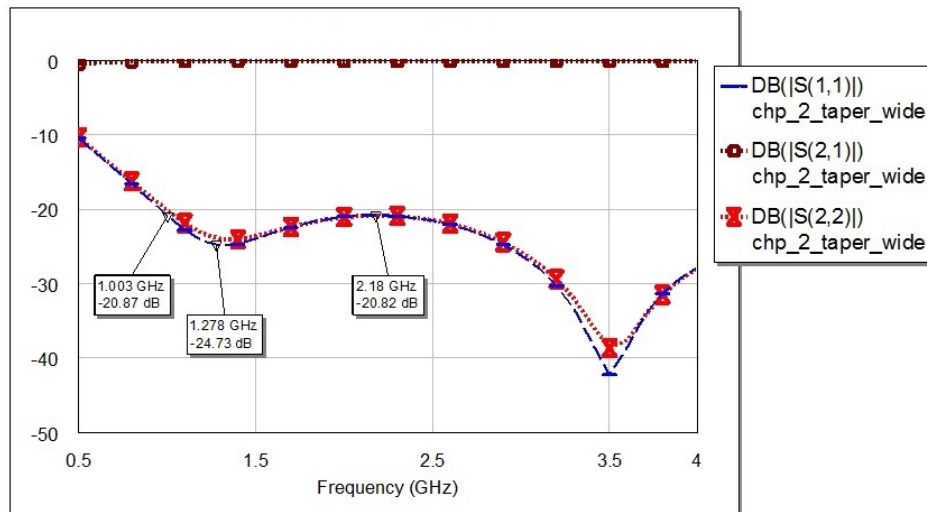


Figure 2.13: Simulation result of the new tapered line from 0.5 GHz to 4 GHz.

# Chapter 3

## Analysis of Isolation Resistors

### 3.1 Equal power dissipation in isolation resistors

This chapter's discussion is based on the odd mode analysis of the  $N$  section Wilkinson divider/combiner. We introduce two main methods in order to determine the isolation resistor values.

The size of the divider has been decided in the even mode. The placement of the isolation resistors are depending on the number of the isolation resistors  $N$ . In order to place the isolation resistors properly, the tapered line is simplified with smaller transmission lines, of which has a  $dx = L/N$  length. The isolation resistors have been added between each transmission line. The structure looks exactly the same as the  $N$  section Wilkinson divider.(Fig. 3.1). All of the different dividers that are introduced in this chapter have the same length  $\bar{L}$  for a fair comparison.

The characteristic impedances of the transmission lines can be extracted from the exponential tapered line design as discussed in the Chapter 2. The characteristic impedances of these transmission lines are  $Z_{even}(x) = Z_{taper}(x)$  at any arbitrary point  $x$ .

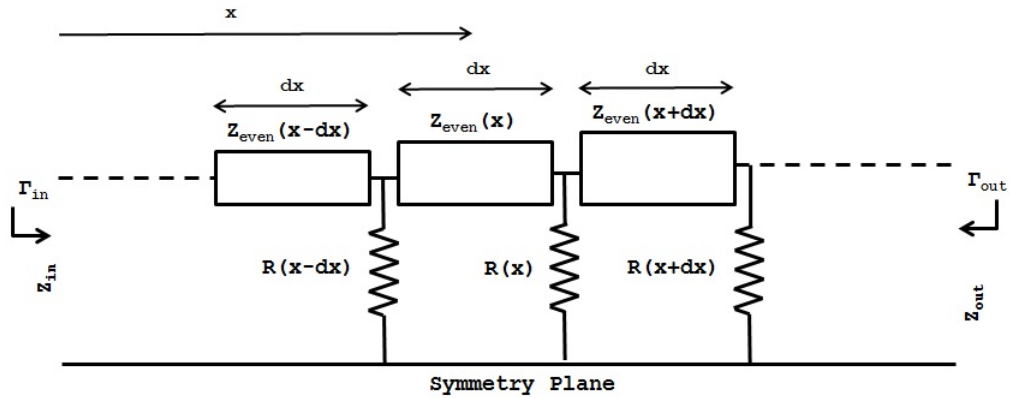


Figure 3.1: The odd mode model of the power divider/combiner with the isolation resistors

Assuming that the two power sources are in phase and combined, the only power loss is going to happen due to the insertion loss, or due to some mismatches at the ports. The desired situation is to make the combined ports less dependent on each other. That is why it is called isolation, which is isolation of two systems. The power that is induced in the odd mode has to be dissipated in the isolation resistors. For example, if 1 Watt power is divided by two and one of the load fails, 0.5W of the power has to be dissipated in the isolation resistors.

The power handling capacity of the power divider/combiner is very important for the high power applications. Single section Wilkinson divider contains only one resistor and its power handling is limited with the package type of the isolation resistor. Most of the standard 0805 package resistors have a power handling capacity of 125mW. The half of the power that is induced to the divider can be dissipated in the isolation resistor in the worst case scenario; therefore, power handling capacity of one section wilkinson power divider with a 0805 package isolation resistor is 250mW. N section power divider contains N resistors and it is very crucial to know which resistor limits the power handling capacity. If any one of the resistors dominates the power dissipation for some frequency range, the power handling capacity of the power/combiner divider is limited by that single resistor, even there are N-1 other resistors. The power should be divided equally over the resistors for all the operating frequency range, thus the power handling capacity can be multiplied by N for identical type of resistors.

The first proposed method regarding the determination of the values of the isolation resistors is based on the equality of the power dissipation on each resistor at the center frequency. Assuming that there are  $N$  resistors and the total power coming in from the port is  $P_{total}$ , the power dissipated in each resistor becomes:

$$P_{resistor} = P_{total}/N \quad (3.1)$$

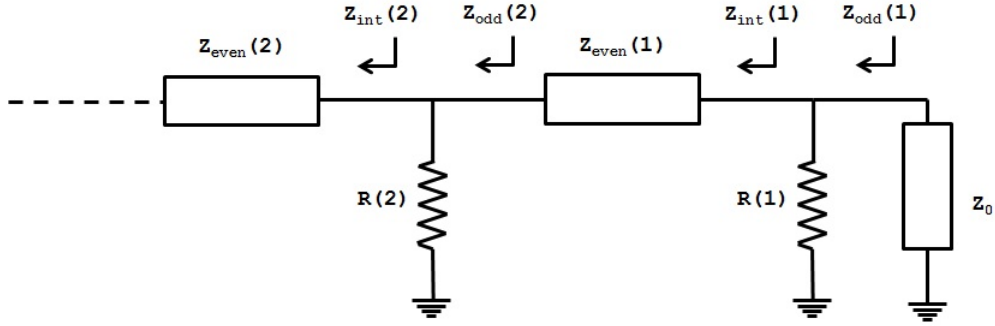


Figure 3.2: First two sections of the  $N$  section power divider in the odd mode.

This assumption provides a simple starting point in order to decide the resistor values on each section. Let us start from the input port in Figure 3.2. There is a shunt resistor  $R(1)$  connected to the input port and there is an impedance that is seen from the rest of the circuit  $Z_{int}(1)$ .  $Z_{odd}(1)$  represents the combination of  $Z_{int}(1)$  and  $Z_{int}(1)$  as follows:

$$Z_{odd}(1) = \frac{Z_{int}(1)R(1)}{Z_{int}(1) + R(1)} \quad (3.2)$$

If the port is perfectly matched, then;

$$Z_{odd}(1) = Z_0$$

Assuming there are  $N$  resistors and the power is equally distributed between them,  $P_{R(1)} = P_{total}/N$  and the rest of the power goes to  $P_{Z_{int}(1)} = (N-1)P_{total}/N$ . Therefore, it is possible to find a relationship between  $Z_{odd}(1)$  and  $R(1)$  as follows,

$$\begin{aligned} NZ_{odd}(1) &= R(1) \\ Z_{int}(1) &= \frac{R(1)}{(N-1)} \end{aligned} \quad (3.3)$$

It is assumed that each intermediate impedance  $Z_{int}(n)$  is real at the center frequency. That is possible when each transmission line section is the quarter wavelength at the center frequency. A quarter wavelength transformer transforms its input and output impedance as follows:

$$Z_{out} = \frac{Z_0^2}{Z_{in}} \quad (3.4)$$

Where  $Z_0$  is the characteristic impedance of the transmission line. In order to calculate the next  $Z_{odd}(2)$ , we use the same equation with a transmission line characteristic impedance  $Z_0 = Z_{even}(1)$  and an input impedance  $Z_{in} = Z_{int}(1)$  thus the equation becomes:

$$Z_{odd}(2) = \frac{Z_{even}(1)^2}{Z_{int}(1)} \quad (3.5)$$

The same process can be repeated for the second section.  $1/N$  percent of the power is already dissipated in the first resistor. Remaining power is  $P_{N-1} = (N-1)P_{total}/N$  and  $P_{N-1}/(N-1) = P_{R(2)}$  and  $P_{Z_{int}(2)} = (N-2)P_{R(2)}$ . Thus,

$$(N-1)Z_{odd}(2) = R(2)$$

$$Z_{int}(2) = \frac{R(2)}{(N-2)} \quad (3.6)$$

Now we can expand the given for any arbitrary  $N$  section structure (equations from 3.2 to 3.6).

$$n = 1, 2, 3 \dots N$$

$$R(n) = (N+1-n)Z_{odd}(n) \quad (3.7)$$

$$Z_{int}(n) = R(n)/(N-n) \quad (3.8)$$

These equations are depending on  $Z_{odd}(n)$  and this can be calculated as another series also as follows:

$$n = 2, 3, \dots, N$$

$$Z_{odd}(n) = Z_{even}(n-1)^2 / Z_{int}(n-1) \quad (3.9)$$

$$Z_{odd}(1) = Z_0$$

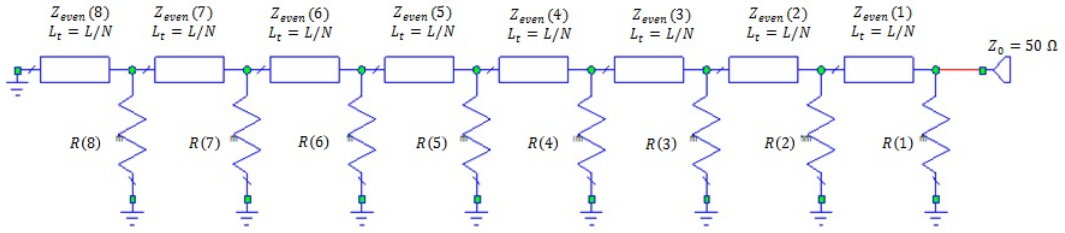


Figure 3.3: The odd mode schematic of the  $N = 8$  section power divider/combiner

Now, it is possible to look to a problem with  $N = 8$  section power divider design with  $Z_0 = 50\Omega$ . (Fig 3.3) The resistors can be calculated with the given equations. Table 3.1 gives the calculated results for the resistor values.

Table 3.1: The isolation resistors and the intermediate impedances for the  $N = 8$  section divider in the odd mode

n	$Z_{even}(n)$ ( $\Omega$ )	$R(n)$ ( $\Omega$ )	$Z_{odd}(n)$ ( $\Omega$ )	$Z_{int}(n)$ ( $\Omega$ )
1	54.00	400.00	50.00	57.14
2	58.33	357.25	51.04	59.54
3	63.00	342.82	57.14	68.56
4	68.04	289.40	57.88	72.35
5	73.49	255.94	63.99	85.31
6	79.37	189.90	63.30	94.95
7	85.72	132.69	66.35	132.69
8	92.58	55.38	55.38	$\infty$

Instead of simulating every different number of  $N$ , it is possible to write the reflection as a function of normalized wavelength  $\theta$ . Assuming that the each section of the transmission line has equal length  $l = L/N$ :

$$\theta = \beta l \quad (3.10)$$

where  $\beta = \frac{2\pi}{\lambda}$  and  $\lambda = v/f$ .  $v$  is the speed of light in the medium and  $f$  stands for the frequency. For instance, if  $\theta = \pi/2$  then  $\lambda = \lambda_c/4$  where  $\lambda_c$  is the



wavelength at the specific frequency  $f_c$ . In other words,  $f_c$  is the frequency where the transmission line is a quarter wavelength.

We place  $\theta$  to the transmission line expression as:

$$Z_{in} = Z_0 \frac{Z_L + jZ_0 \tan(\theta)}{Z_0 + jZ_L \tan(\theta)} \quad (3.11)$$

The reflection from the port may be written as:

$$\Gamma = \frac{Z_{odd}(1) - Z_0}{Z_{odd}(1) + Z_0} \quad (3.12)$$

Beginning from the  $N$ th section of the given odd mode structure, we can calculate each section's odd mode impedance with an iterative approach as follows:

$$Z_{int}(n) = Z_{even}(n) \frac{Z_{odd}(n+1) + jZ_{even}(n)\tan(\theta)}{Z_{even}(n) + jZ_{odd}(n+1)\tan(\theta)} \quad (3.13)$$

$$Z_{odd}(n) = \frac{Z_{int}(n)R(n)}{Z_{int}(n) + R(n)} \quad (3.14)$$

In the first equation  $Z_{int}(n)$  depends on  $Z_{odd}(n+1)$ . Therefore it is necessary to calculate  $Z_{odd}$  or  $Z_{int}$  from  $n = N$  to  $n = 1$ . While the last node is a short circuit due to the odd mode:

$$Z_{odd}(N+1) = 0$$

Now it is possible to calculate the reflection as a function of  $\theta$ . By using the resistor values for different  $N$  section network, we can calculate  $\Gamma(\theta)$  for  $0 \leq \theta \leq \pi$ .

Figure 3.4 shows the input reflection for different  $N$  section designs. While our calculations are based on a perfect matching at the center frequency, at  $\theta = \pi/2$  the reflection is minimum. As the number of sections increases, the bandwidth also increases. The equal power dissipation at the center frequency is a sufficient analytical assumption to calculate the intermediate resistors. The equally power dissipating resistor values and the achievable bandwidth are given in Table 3.2 for some  $N$  section divider/combiners.

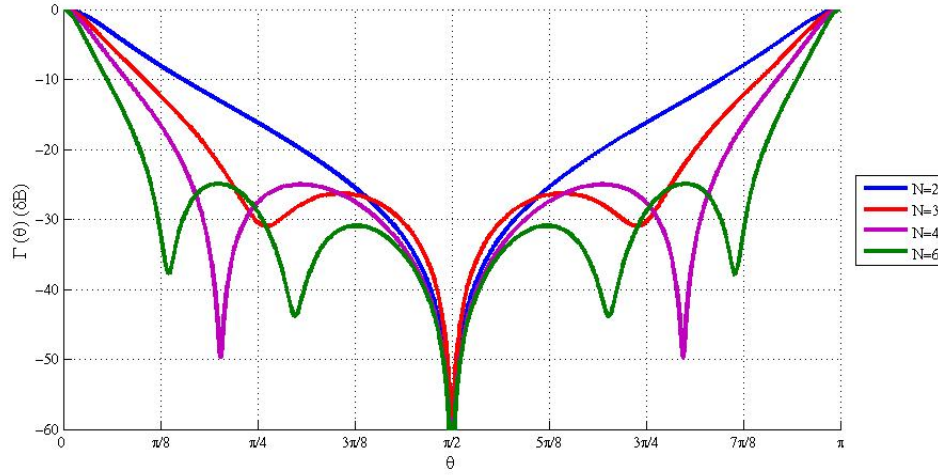


Figure 3.4: The reflection of the  $N$  section divider with equally power dissipating resistors in the odd mode

Table 3.2: Equally power dissipating resistor values and the bandwidth for the  $N$  section power divider

<b>N</b>	<b>2</b>	<b>3</b>	<b>4</b>	<b>6</b>	<b>8</b>
<b>BW (-20dB)</b>	2.26	4.36	5.94	9.17	12.31
<b>R1</b>	100	150	200	300	400
<b>R2</b>	39.68	94.28	148.44	253.96	357.25
<b>R3</b>		53.03	117.29	234.05	342.82
<b>R4</b>			48.97	174.14	289.40
<b>R5</b>				126.81	255.94
<b>R6</b>				53.07	189.90
<b>R7</b>					132.69
<b>R8</b>					55.38

## 3.2 Linear variation for the isolation resistors

The second method to determine the values of the isolation resistors has been found empirically. Assuming the input impedance of the  $N$  section divider is  $Z_0$ , isolation resistors can be chosen as:

$$R(n) = (N + 1 - n)Z_0 \quad (3.15)$$

Table 3.3 provides the resistor values for different  $N$  section linearly changing resistor values and observed bandwidth for -20 dB level. The linear decision

option for the resistor values harms the isolation bandwidth slightly for  $N \geq 3$ . Additionally, it is not guaranteed that all resistors are equally power dissipating. However, this choice will make implementation very easy

Table 3.3: The resistor values decided with linear variation and the bandwidths for the different  $N$  section power dividers

<b>N</b>	<b>2</b>	<b>3</b>	<b>4</b>	<b>6</b>	<b>8</b>
<b>BW (-20dB)</b>	2.8	4.3	5.75	8.66	11.57
<b>R1</b>	100	150	200	300	400
<b>R2</b>	50	100	150	250	350
<b>R3</b>		50	100	200	300
<b>R4</b>			50	150	250
<b>R5</b>				100	200
<b>R6</b>					150
<b>R7</b>					100
<b>R8</b>					50

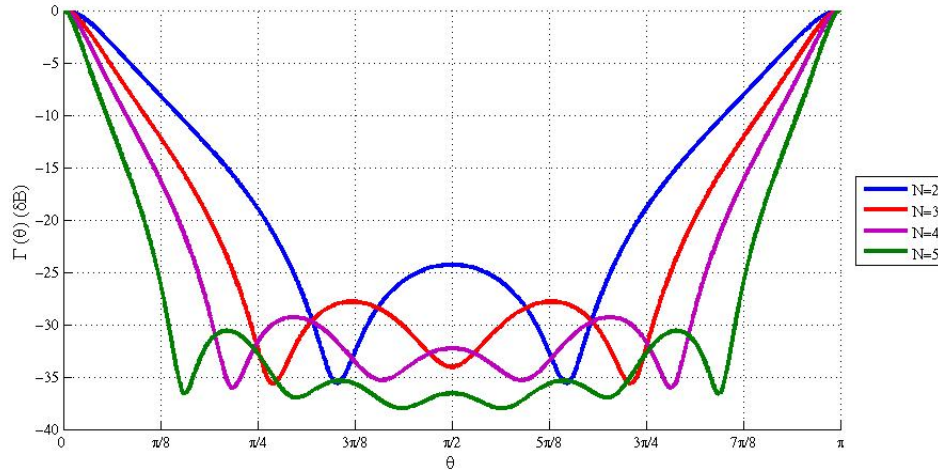


Figure 3.5: The reflection of the  $N$  section dividers with the linear decision option in the odd mode

Consequently, it has been shown that the determination of the isolation resistor value can be done in two ways. The first option is based on equal power dissipation. The second option is the linear variation. Table 3.2 and Table 3.3 show different possible bandwidths and resistor values for both of these options. While the linear variation option is simpler than the equal power dissipation option, the linear variation option has a slightly smaller bandwidth for  $N \geq 3$ .

### 3.3 Bandwidth improvement of the isolation

It is possible to improve the bandwidth for both of the methods. The total wavelength of the tapered line can be calculated as a function of  $\theta$ .  $\theta = \beta l$  where  $\beta = 2\pi/\lambda$  and  $l = L/N$ , then:

$$\theta = \frac{2\pi L}{N\lambda} \quad (3.16)$$

$\lambda_1$  is the wavelength of  $f_1$  and it is desired that is  $4\lambda_1 = L$ .

$$\theta_1 = \pi/2N$$

On the other hand, it is known that each transmission line section with the length  $l$  is quarter wavelength at the center frequency  $f_c$ , thus  $4\lambda_c = l$ .

$$\theta_c = \frac{2\pi l}{\lambda_c}$$

$$\theta_c = \pi/2$$

The higher limit can be written as:

$$\theta_2 = \theta_c + (\theta_c - \theta_1) = 2\theta_c - \theta_1 \quad (3.17)$$

The target bandwidth can be calculated as:

$$BW_{target} = \frac{\theta_2}{\theta_1} = \frac{2\theta_c - \theta_1}{\theta_1} = \frac{2\theta_c}{\theta_1} - 1 = \frac{\pi}{\pi/2N} - 1$$

$$BW_{target} = 2N - 1 \quad (3.18)$$

As an example, a divider with  $N = 8$  section, the target bandwidth is  $BW_{target} = 15$ . The given results for the previous options are not able to reach that limitation. It has been experimentally observed that the first resistor  $R(1)$  has the most significant effect on the lowest frequency. The new resistor value  $R'(1)$  is defined with an improvement factor of  $\delta$ :

$$R'(1) = \frac{R(1)}{\delta} \quad (3.19)$$

$\delta$  can be found with simulations for different  $N$  section designs. Fig. 3.7 displays the improved reflections of the different  $N$  sections with the resistors that are

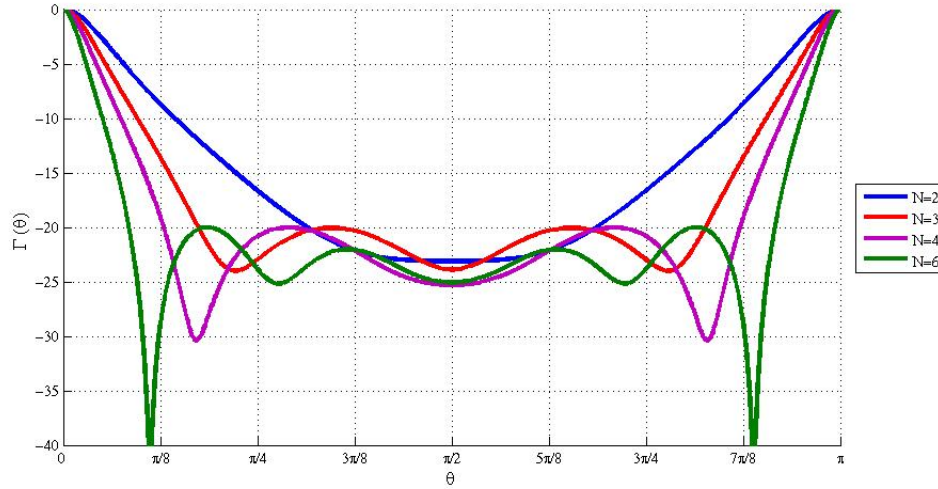


Figure 3.6: The reflection of the  $N$  section divider with the improved equal power dissipation option in the odd mode

calculated with the linear variation option. Fig. 3.6 displays the improved reflections of different  $N$  sections with the resistors that are calculated with equal power dissipation option.

Now, we have two main options and two improved versions of these main options in order to determine the isolation resistors. Table 3.4 shows the bandwidth results of these four options and  $\delta$  values.  $N$  section Wilkinson power divider is limited by the even mode. We show the  $N$  section Chebyshev matched Wilkinson divider bandwidth for comparison.

Each option for the resistors has its own advantage. For instance, the linear option is very easy to use and its bandwidth can be very easily improved by lowering the first resistor value. On the other hand, the equal power has the best power handling performance since, the power dissipates on each of the resistors equally. The bandwidth improvement of the equal power option ruins the equal power dissipation condition, yet it gives the best bandwidth result for  $N \geq 4$ .

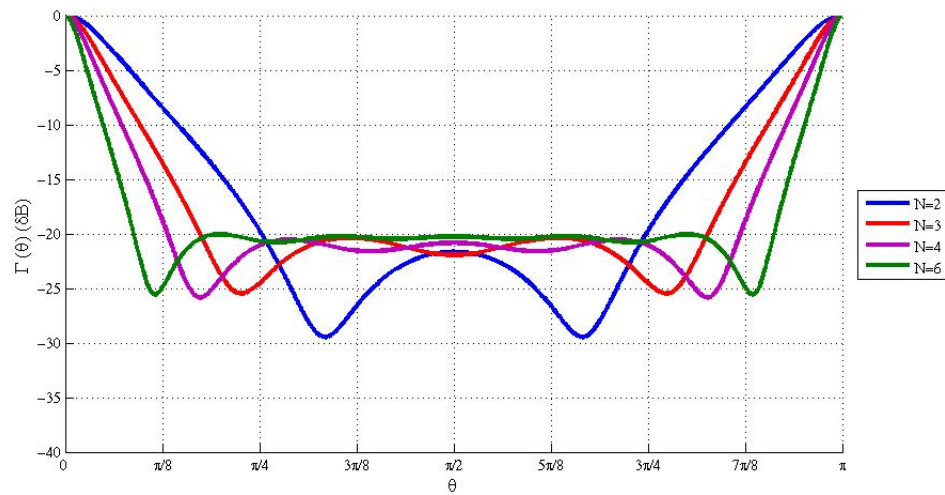


Figure 3.7: The reflection of the  $N$  section divider with the improved linear variation option in the odd mode

Table 3.4: Bandwidth comparisons of different resistor decision methods with different  $N$

N	Linear variation method		Equal power dissipation method			Literature		
	BW (-20 dB)	$\delta$	BW with $\delta$ (-20 dB)	BW (-20 dB)	$\delta$	BW with $\delta$ (-20 dB)	Chebyshev based Wilkinson BW (-20dB)	Cohn's BW (-25 dB)
2	2.8	1.1	2.96	2.26	1.13	2.33	2.75	2
3	4.3	1.4	4.76	4.36	1.41	4.76	4.25	3
4	5.75	1.6	6.6	5.94	1.46	6.76	5.8	4
5	7.2	1.89	8.5	7.63	1.62	8.92	7.4	-
6	8.66	2.11	10.39	9.17	1.71	10.85	9	-
7	10.1	2.34	12.31	10.77	1.82	12.84	10.59	10
8	11.57	2.57	14.18	12.31	1.91	14.71	12.21	-
9	13.03	2.79	16.08	13.89	2	16.55	13.83	-
10	14.48	3.02	18.04	15.37	2.08	18.39	15.46	-
11	15.98	3.22	19.95	16.95	2.17	20.23	17.06	-
12	17.38	3.47	21.78	18.4	2.25	22.1	18.76	-
13	18.88	3.69	23.74	19.95	2.33	23.75	20.37	-
14	20.23	3.92	25.64	21.45	2.4	25.63	21.94	-

Lastly, it is possible to compare the results on Figure of Merit that is defined in Chapter 1.  $L$  and  $\bar{L}$  can be written as:

$$\begin{aligned} L &= \lambda_c N / 4 \\ \bar{L} &= \frac{\lambda_c N}{4\lambda_1} \end{aligned} \quad (3.20)$$

Now, we need to calculate  $\lambda_c$  and we know that  $\theta_c = \pi/2$ .

$$\begin{aligned} \theta &= \beta l = \frac{2\pi}{\lambda} l \\ \lambda_c &= 4l \end{aligned}$$

It is necessary to calculate  $\lambda_1$  and it can be derived from the  $BW$  as follows:

$$\begin{aligned} BW &= \theta_2 / \theta_1 \\ \theta_2 &= BW \theta_1 \\ \theta_c &= \frac{\theta_2 + \theta_1}{2} \\ \theta_2 + \theta_1 &= \pi \\ \theta_1 &= \frac{\pi}{BW + 1} \\ \lambda_1 &= \frac{2\pi}{\theta_1} l \\ \lambda_1 &= 2(BW + 1)l \end{aligned} \quad (3.21)$$

Using calculated  $\lambda_1$  and  $\lambda_c$ :

$$\bar{L} = \frac{N}{2(BW + 1)}$$

Therefore, FoM can be written as:

$$\begin{aligned} FoM &= \frac{BW}{\bar{L}} \\ FoM &= \frac{2BW(BW + 1)}{N} \end{aligned} \quad (3.22)$$

Table 3.5 gives the  $FoM$  and  $\bar{L}$  results for the given bandwidths.



Table 3.5: Figure of merit and  $\bar{L}$  results of different resistor decision methods

N	Linear variation method		Improved BW linear variation method		Equal power dissipation method		Improved BW equal power dissipation method		Chebychev based Wilkinson		Cohn	
	$L$	FoM	$L$	FoM	$L$	FoM	$L$	FoM	$L$	FoM	$L$	FoM
2	0.23	14.36	0.22	16.24	0.26	10.73	0.25	11.54	0.27	10.31	0.3	6.00
3	0.25	20.06	0.23	25.10	0.25	20.57	0.23	25.01	0.29	14.88	0.4	8.00
4	0.26	25.68	0.23	34.53	0.26	26.78	0.22	36.92	0.29	19.72	0.4	10.00
5	0.27	31.44	0.23	43.91	0.26	33.76	0.21	49.55	0.30	24.86	-	-
6	0.27	37.11	0.23	53.73	0.26	39.73	0.21	61.48	0.30	30.00	-	-
7	0.28	42.63	0.23	63.42	0.27	46.05	0.21	72.67	0.30	35.07	0.3	31.43
8	0.28	48.36	0.23	73.48	0.27	52.26	0.21	83.85	0.30	40.32	-	-
9	0.28	54.11	0.23	83.46	0.27	58.39	0.21	96.77	0.30	45.58	-	-
10	0.28	59.51	0.23	93.49	0.27	64.62	0.21	106.89	0.30	50.89	-	-
11	0.28	65.70	0.23	103.43	0.27	70.14	0.21	117.88	0.30	56.02	-	-
12	0.28	70.64	0.23	111.86	0.27	75.76	0.21	128.82	0.30	61.78	-	-
13	0.29	76.30	0.23	121.20	0.28	82.23	0.21	138.56	0.30	66.97	-	-
14	0.29	82.57	0.23	131.24	0.28	88.10	0.21	151.54	0.31	71.90	-	-

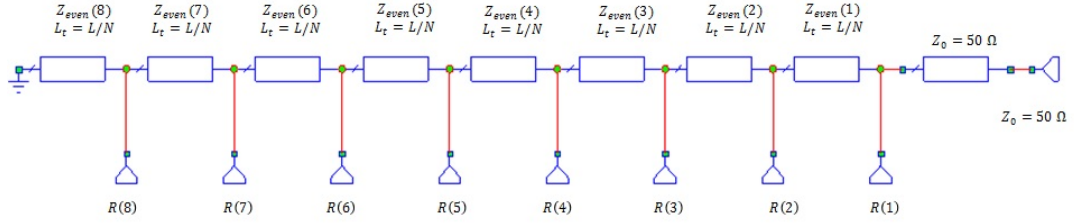


Figure 3.8: Schematic model of odd mode where resistors have been replaced with ports.

### 3.4 Power handling capacity of the proposed methods

In order to find which resistor is more power consuming than the others, we should consider each resistor as a port so that each port has the impedance of the resistor that is replaced (Fig. 3.8). The input reflection which is expected for the original port will be exactly the same as the real resistor case. The power injected from the original port (that is port 1 in our case) transferred to other ports (port  $n$  which is any other port rather than 1).  $S(n,1)$  gives the value of power injected to the resistor  $n$ .

In our case, we already have four different options to determine the resistor values. This should not effect the response and we should be able to add the last resistor as a port. Figure 3.9 shows the power dissipation of the resistors when the linear variation decision option is used. Figure 3.10 shows the equal power dissipation method, Figure 3.11 shows the bandwidth improved linear variation method and Figure 3.12 shows the bandwidth improved equal power dissipation method power dissipation in the isolation resistors. Lastly, Figure 3.13 shows an eight section bandwidth optimized Wilkinson power divider's power dissipation in the isolation resistors.

The desired result is that the power dissipation among resistors is equal over a certain frequency band. If the power comes from the port which is distributed to

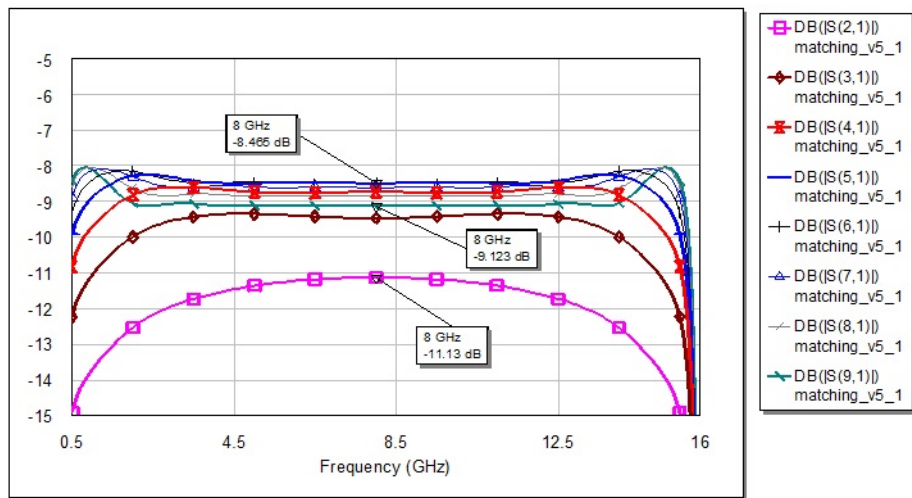


Figure 3.9: Power dissipation results of the resistors for the linear variation method

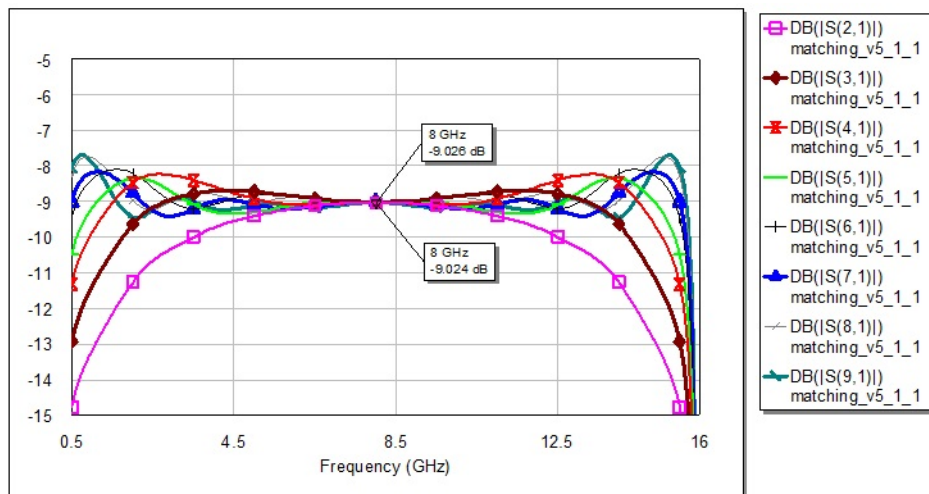


Figure 3.10: Power dissipation results of the resistors for the equal power dissipation option

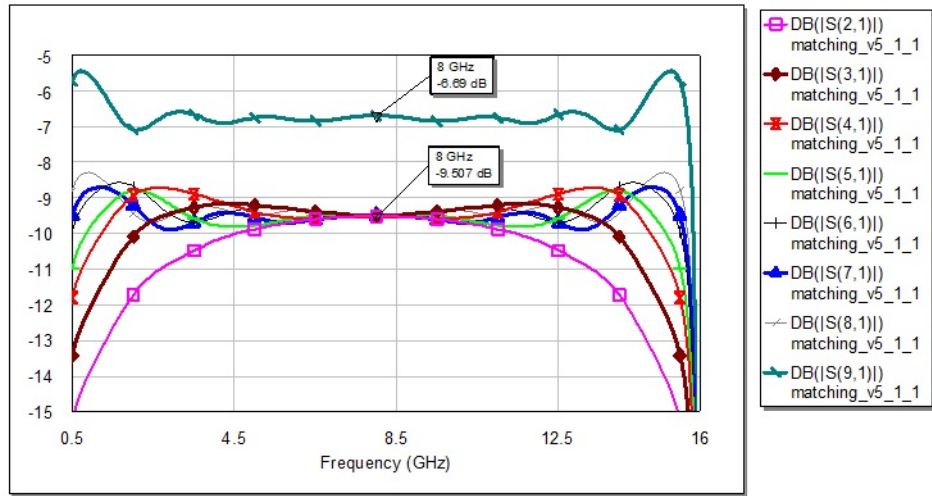


Figure 3.11: Power dissipation results of the resistors for the bandwidth improved equal power dissipation option

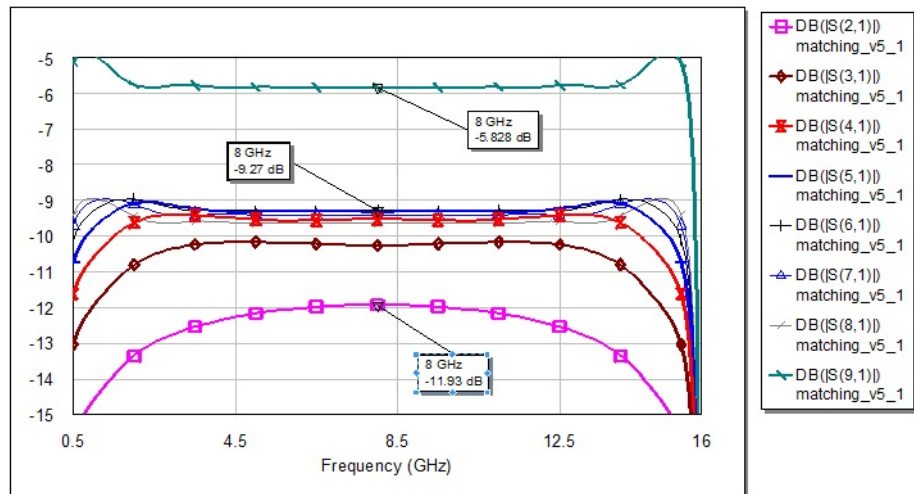


Figure 3.12: Power dissipation results of the resistors for the bandwidth improved linear resistor decision option

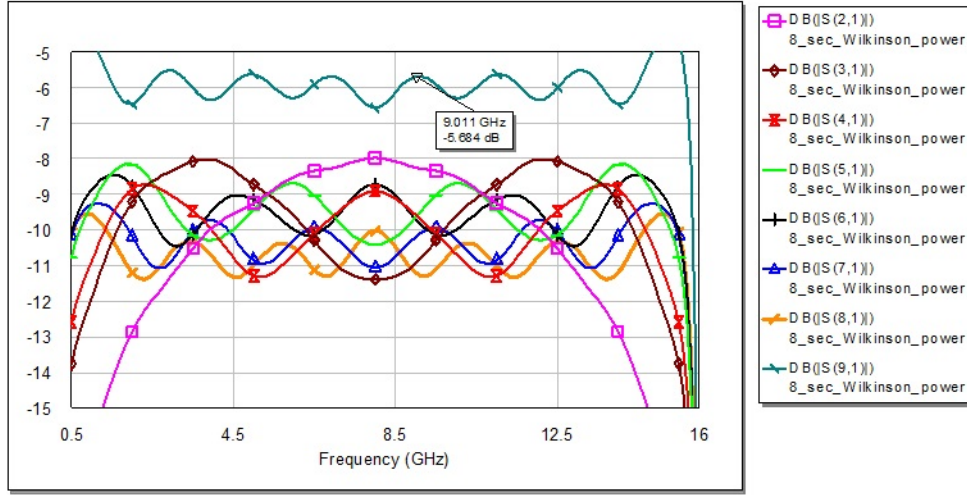


Figure 3.13: Power dissipation results of the resistors for the optimized Wilkinson resistors

the resistors equally,  $dB S(n, 1) = 10 \log(1/N)$ . If number of sections is  $N = 8$ , then the expected S-parameters is  $dB S(n, 1) = -9.03$  dB. The results show that the equal power dissipation option achieves equal power dissipation sufficiently at the center frequency (Figure 3.11). The linear option has a similar result; however, the last resistor receives slightly less power than other resistors. On the other hand, for other options including the optimized eight section Wilkinson, the power is not dissipated equally and the  $R(1)$  dissipates approximately 0.25 of the incoming power (Figure 3.13). Thus, the power handling capacity of the improved options and the optimized Wilkinson design is half of the equal power option.

Assuming that the power handling capacity of each resistor of the divider is  $P_{resistor}$ , the total power handling capacity of the divider can be written as:

$$P_{divider} = \gamma P_{resistor}$$

where  $\gamma$  depends on  $N$ . The desired situation for the best handling capacity is  $\gamma = N$ . However, it has been shown that power handling capacity of the divider is not at the desired levels if the resistors are not chosen properly. Table 3.6 shows  $\gamma$  results for the aforementioned methods. Table 3.5 shows that the bandwidth improvements of the proposed methods reduces the power handling capacity of

the given methods significantly. The equal power option gives the best power handling performance.

Table 3.6:  $\gamma$  values of the different resistor decision methods with different  $N$

<b>N</b>	<b>Linear variation method</b>	<b>BW imp. Linear var.</b>	<b>Equal power</b>	<b>BW imp. Equal power</b>
<b>2</b>	1.79	1.87	2	1.89
<b>3</b>	2.94	2.51	3	2.42
<b>4</b>	3.73	3	4	3.06
<b>5</b>	4.48	3.19	5	3.47
<b>6</b>	5.36	3.45	6	3.92
<b>7</b>	6.2	3.63	7	4.3
<b>8</b>	7.02	3.79	8	4.67
<b>9</b>	7.82	3.92	9	5
<b>10</b>	8.68	4.04	10	5.33
<b>11</b>	9.49	4.15	11	5.61
<b>12</b>	10.3	4.21	12	5.89
<b>13</b>	11.12	4.29	13	6.15
<b>14</b>	11.96	4.35	14	6.42

# Chapter 4

## A Quarter Wavelength Tapered Power Divider/Combiner

### 4.1 Tapered power divider/combiner design

In previous sections, the even mode and the odd mode analyses have been discussed. Now, it is time to combine these two structures and see the result in the schematic model. Both symmetric sides contain a capacitance at the input side. Instead of adding two capacitors, it is more practical to combine two capacitors. The isolation resistors are also doubled. The isolation resistor values have been determined according to the improved linear decision option explained in Chapter 3. The schematic structure of the power divider is given in Figure 4.1.

The expected result is a combination of the odd mode and the even mode analyses. In accordance with the symmetry, all of the insertion S-parameters decrease 3 dB. ( $S_{21}$ ,  $S_{23}$ , etc.). The resulting simulation shows that it is possible to achieve a good bandwidth by using the combined structure. (Fig. 4.2)

While the designed power divider is ready in the schematic model, it is beneficial to compare these results to a known structure, which is the N section

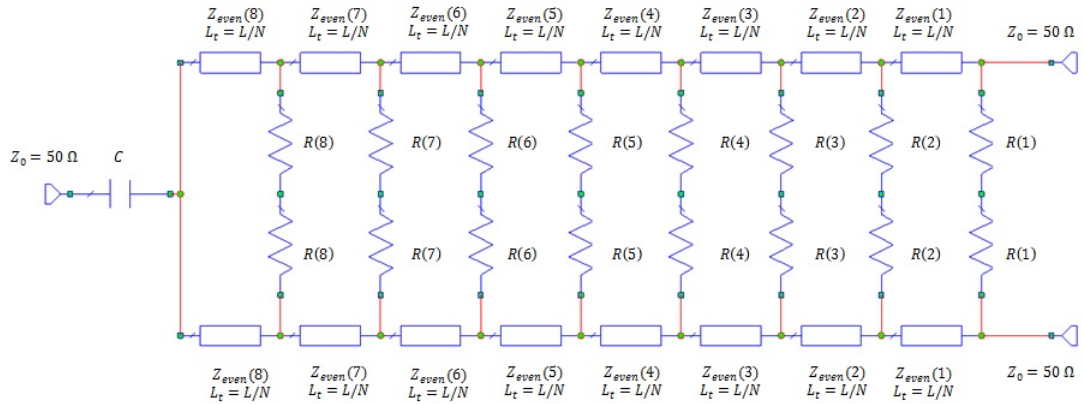


Figure 4.1: Schematic model of the new tapered power divider/combiner design.

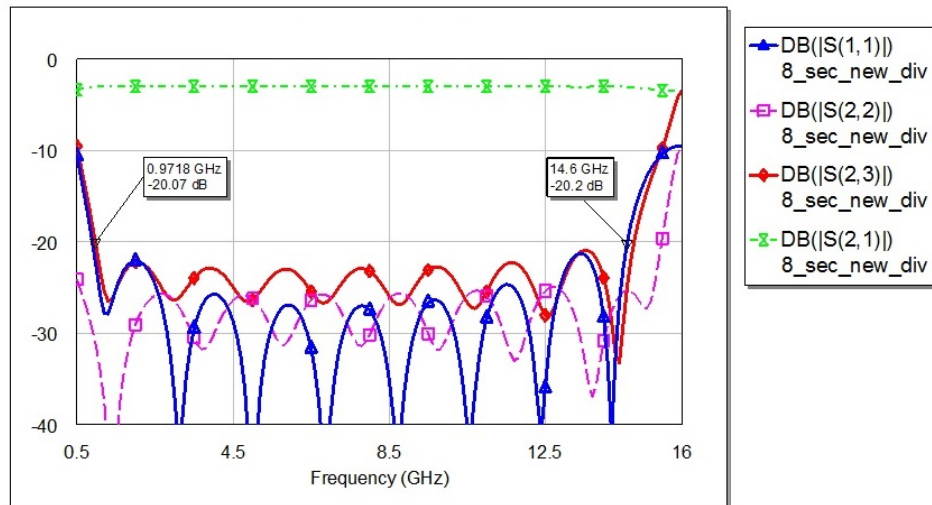


Figure 4.2: S-parameter simulation results of the new power divider design



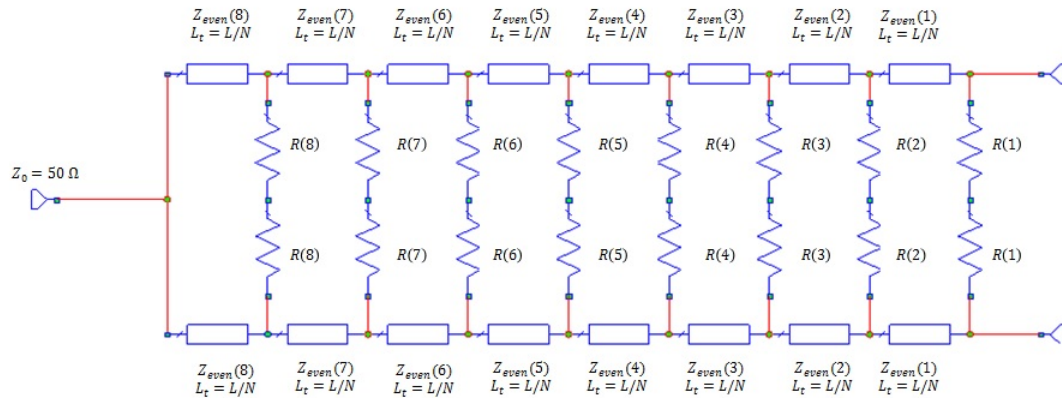


Figure 4.3: Schematic model of eight section Wilkinson power combiner divider design.

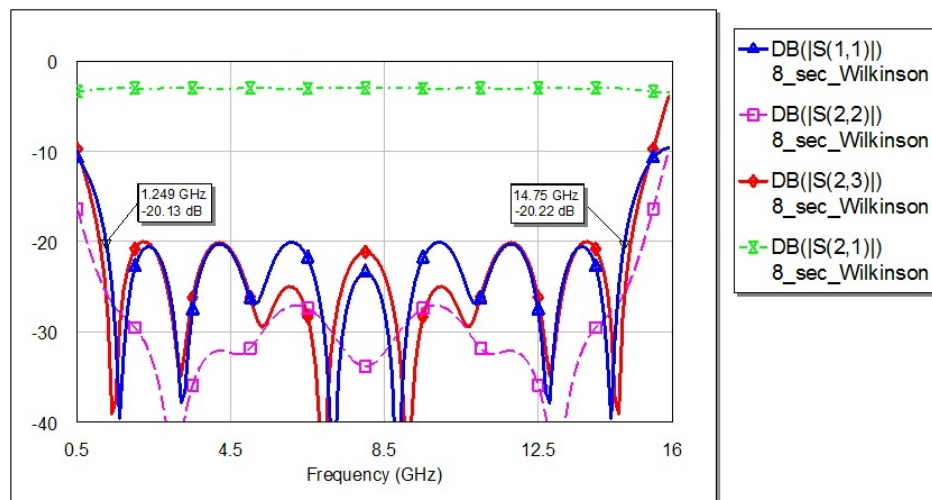


Figure 4.4: S-parameter simulation results of the eight section Wilkinson power divider design

Wilkinson power divider. In Cohn's paper, the seven section power divider/combiner gives the bandwidth  $f_2/f_1 = 10$  [3]. The resulting bandwidth of Wilkinson divider is approximately  $f_1/f_2 = 11.3$  ( $N = 8$ ). (Fig. 4.4) Our design has a bandwidth ratio of  $f_2/f_1 = 15$  ( $N = 8$ ). (Fig. 4.2)

## 4.2 EM model of the new power divider/combiner design

The desired structure is given in Figure 4.5. The implementation of the EM model is not easy as the schematic model. There is a matching problem at the input side. There are two transmission lines connected to the input port that is  $50 \Omega$ . In our calculations in Chapter 2,  $100 \Omega$  line is approximately  $0.3 \text{ mm}$  and  $50 \Omega$  line is  $1.1 \text{ mm}$ . Two of the  $100 \Omega$  lines, which are adjacent to each other, make a total of  $0.6 \text{ mm}$  width and they will be connected to a  $1.1 \text{ mm}$  ( $50 \Omega$ ) input line. There is a step change of the transmission line where it is not very easy to implement in the schematic model. Additionally, the gap between tapered lines is quite small. This causes the second implementation problem. When two lines get closer to each other, they start to couple and their impedances differ for the odd mode and the even mode [1]. These problems have been left to be solved in the EM optimization.

It is possible to place chip resistors for the isolation. However, instead of placing the discrete resistors, surface resistive materials (Ohmic sheet) have been used. These materials are very commonly used in standard chip resistors that are built in a thin film or a thick film processes. The ohmic sheet materials have a surface resistivity constant of  $\rho$  ( $\Omega/\text{sq}$ ). When it is necessary to build a rectangular shaped resistor with this material, the formulation is simply  $R = \rho A/B$  where  $A$  is the length of the resistor and  $B$  is the width of the resistor.

It is not very easy to show the RF response of different sized resistors. Commonly, smaller the resistor's size is, better the frequency response is. There are also other methodologies to show the frequency response of discrete resistors, such

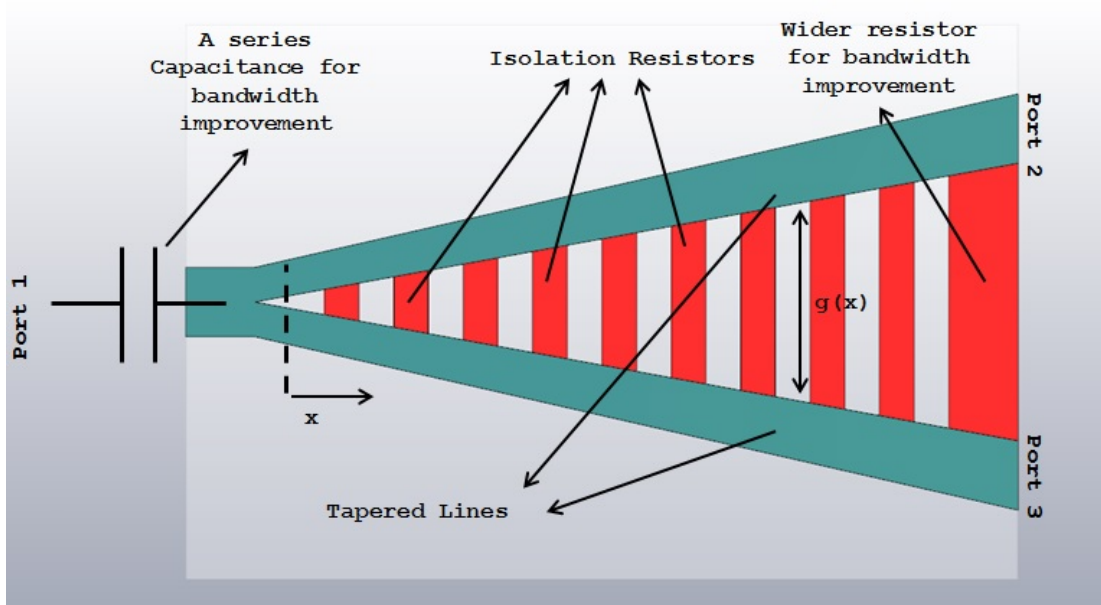


Figure 4.5: The designed combiner/designer with the discrete resistors.

as defining its lumped element models or modeling it with a very lossy transmission line. However, these models are very dependent on the substrate and the placement of the resistor. The resistors that are used in this section will be as small as possible.

These surface resistive materials do not have a very wide range of  $\rho$ . The most common and easy to find material is  $50 \Omega/\text{sq}$  and its multiples such as  $100 \Omega/\text{sq}$ ,  $200 \Omega/\text{sq}$  etc. Manufacturers of discrete resistors can use different techniques such as laser trimming to produce any value of resistance or any arbitrary shape, but these methodologies are not being used in this thesis.

The resistor values have been calculated in Chapter 3 with the improved linear variation option. Each resistor is implemented as a rectangular shape and placed in the gap. The gap between tapered lines is implemented as a function  $G = At^2 + Bt$  where  $t$  is from 0 to 1. The real length of the line is 46 mm. The gap is  $G = A + B$  at the end of tapered lines, since  $t = 1$ . The length is also a function of  $t$  and it is simply  $L = 46 * t$ . It is known that the increase in the resistor is linear, therefore, the second order is not necessary  $A = 0$ . The widths of the resistors have been chosen 0.1 mm. The first resistor have a slightly larger

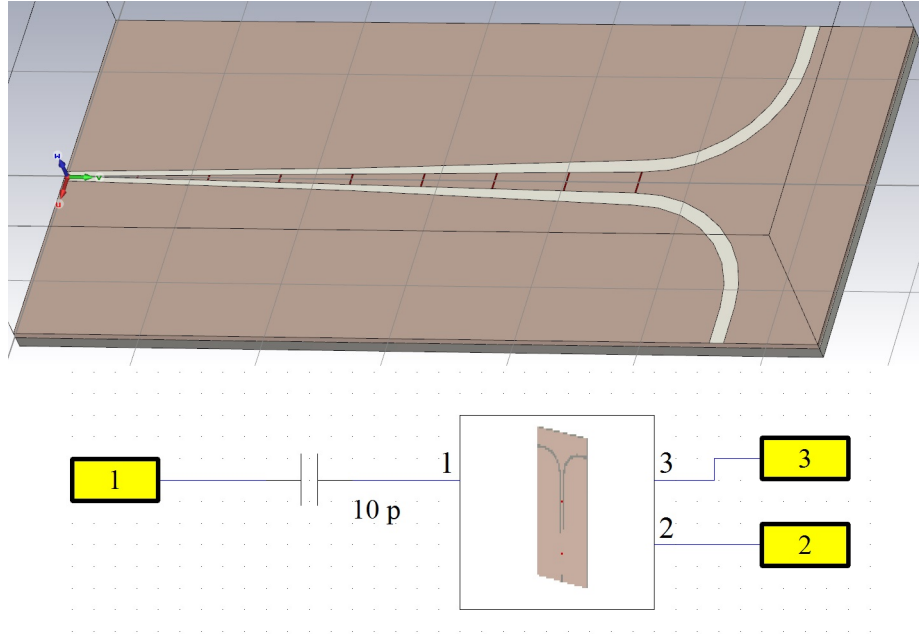


Figure 4.6: EM structure of the designed combiner/designer with the discrete resistors.

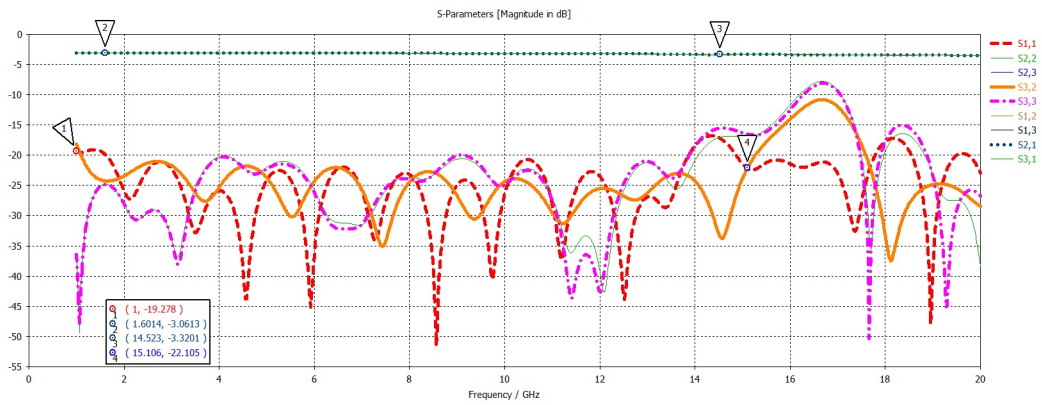


Figure 4.7: EM Simulation of designed power combiner/designer with extended bandwidth.

width to improve the bandwidth. Eight rectangular resistors have been drawn accordingly to the improved linear decision option.

The simulation has been set from 1 GHz to 20 GHz. In order to increase the even mode bandwidth, there is a need for a capacitance at the input side. It is not very practical to add a capacitance in the EM model. They are very hard to implement and the internal structure of the capacitance should also be known. Instead of losing time with redesigning a capacitance for the EM model, a schematic simulation of the CST has been used. (Fig 4.6). The resulting simulation shows that it is possible to achieve a very good band response (Fig. 4.7).

### **4.3 Implementation of tapered power divider/-combiner with discrete isolation resistors**

It is very hard to manufacture a 0.1 mm width for the isolation resistors. Thus, simple discrete 0603 packaged resistors have been used to implement the design. The resistors have been chosen according to the improved linear decision option.

The resulting structure is very similar to the EM simulation case. (Fig. 4.8) Higher frequencies have some loss due to the input coupling. We have used coaxial SMA to microstrip end launch connectors to couple the signal. These connectors have a maximum frequency limit which is about 15 GHz. These connectors have a very poor response and have additional loss due to their discontinuities at high frequencies. Figure 4.9 shows that, the main problem with this design is the insertion loss. This loss arises from the non-idealities of resistors.

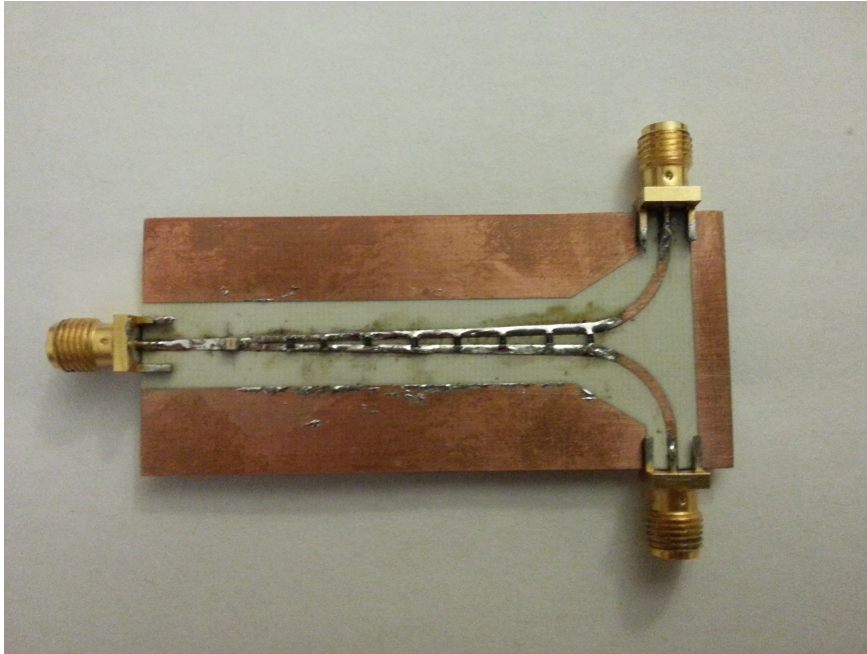


Figure 4.8: Realization of discrete resistor design

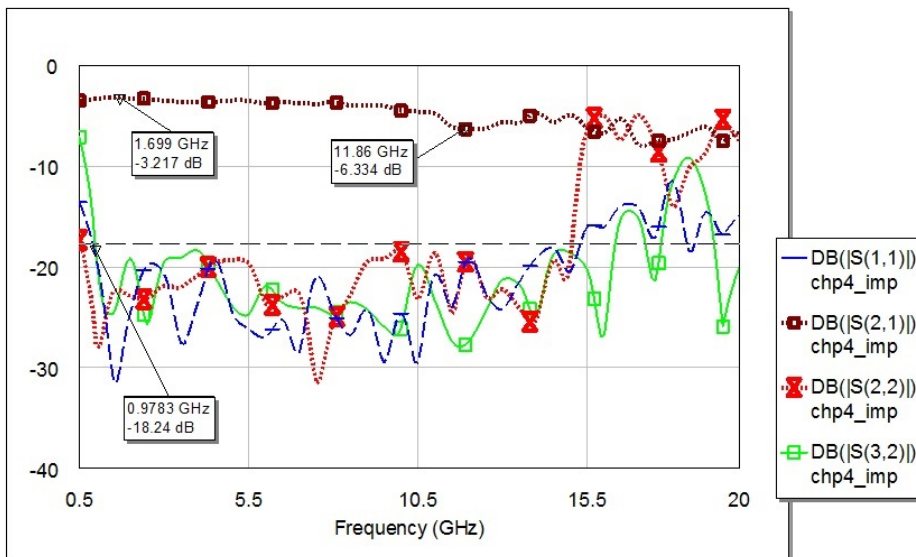


Figure 4.9: Network Analyzer Results of realized design with discrete resistors

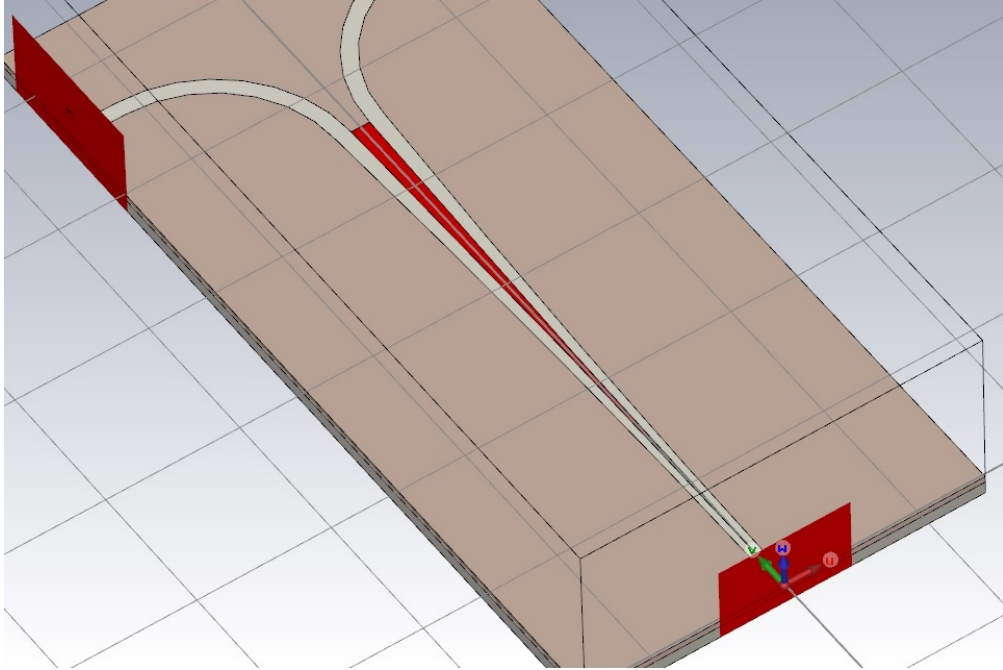


Figure 4.10: EM Model of continuous isolation resistance.

#### 4.4 EM model of the continuous isolation resistor power divider/combiner

In this section the purpose of the design is to achieve a tapered power divider structure similar to Goodman [11](Fig. 4.10). The gap between tapered lines is filled with  $50 \Omega/\text{sq}$  resistive layer and the resulting structure has been simulated. Figure 4.11 shows that the port reflections and the isolation are below  $-15 \text{ dB}$  over most of the frequency range.

There is an obvious insertion loss because of an even mode problem at the higher frequency. In the schematic model, the ideal discrete resistors are connected to the exact symmetrical side of the combiner. However, the continuous resistance or real discrete resistors (as in the previous section) have a real width. This width causes a continuous connection between the tapered lines. While there are multiple connections between the lines, each node has been connected to any other node, where the signal has another phase. In that case, the even mode assumption is refuted. In other words, as a worst case scenario; while the signal's

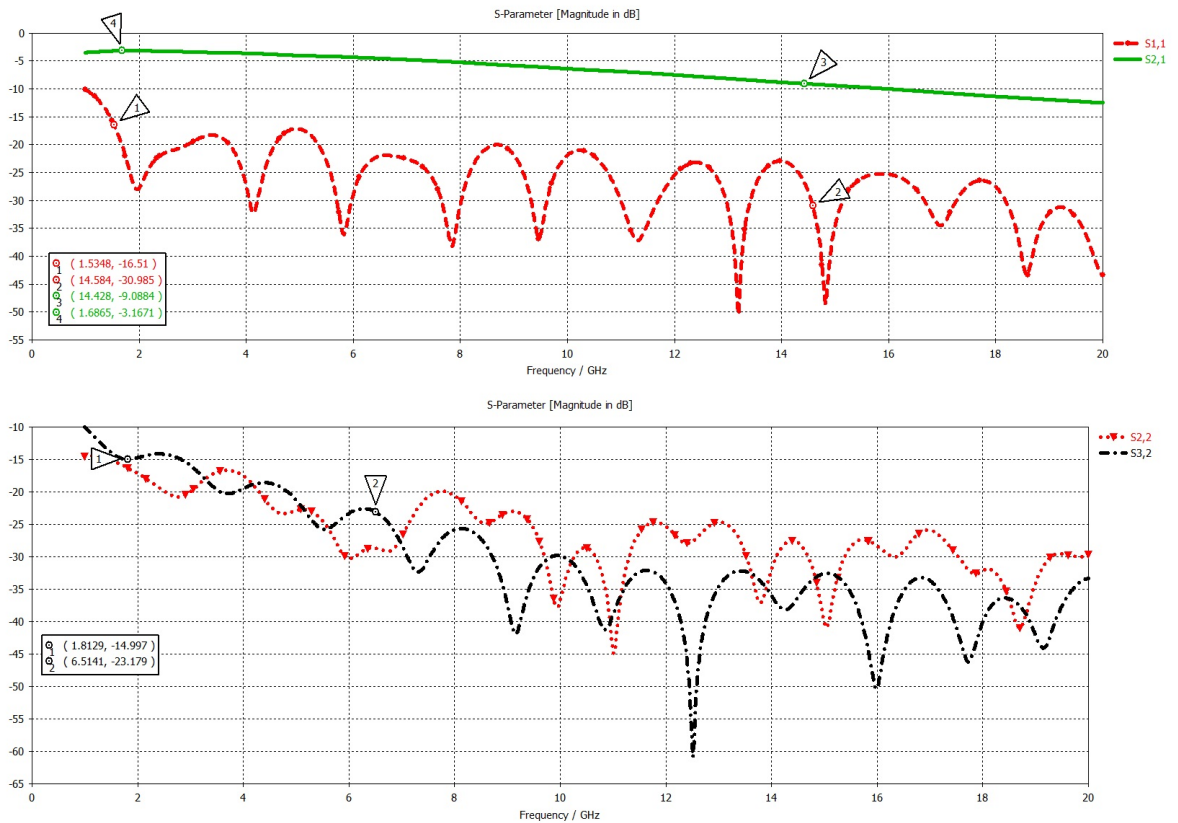


Figure 4.11: EM Simulation of continuous tapered divider with  $50 \Omega/\text{sq}$  surface resistive material

voltage is at the maximum, there is a connection to a node on the other side at which there is a voltage minimum. Some of the power is lost on that highly lossy path (that is a low resistive path). Figure 4.12 gives a visualization of the problem. The current flowing between maximum and minimum points of the standing voltage is the worst case. The connections do not necessarily take place between the highest and the lowest voltages. Any connection in between two different phases means that a voltage difference is going to occur which eventually causes a loss.

In order to prevent the loss, the surface resistivity has been increased to a  $1000 \Omega$  (which means interconnections are highly resistive, and current will not flow between different phases). In order to satisfy the isolation, the gap between tapered lines has been reduced. It might be thought that the gap is smaller and each path for the lossy connections is also smaller, therefore it would not help.



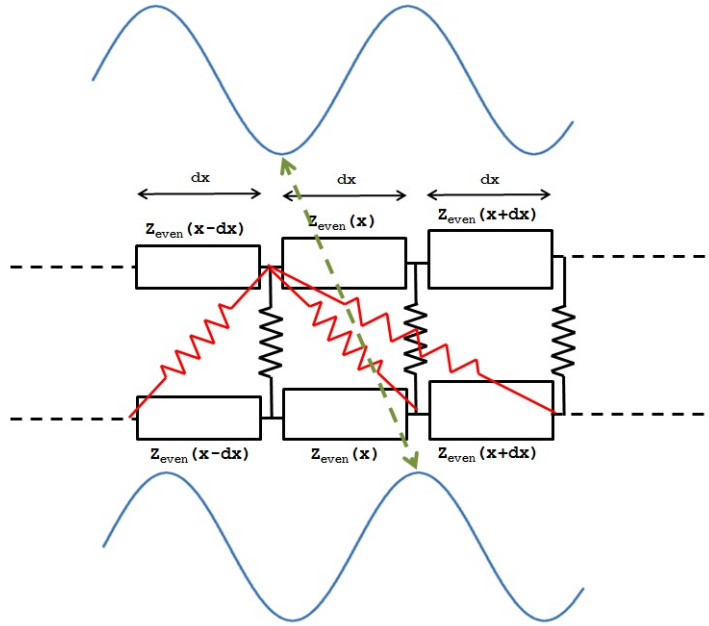


Figure 4.12: Visualization of even mode loss, red resistors are models of continuous resistor, blue waves are signals and green line is the connection between peaks of the signals.

However, the distance between a voltage maximum and a voltage minimum does not change at all (Fig. 4.12). Lengths of the lossy paths are not decreased with the same order and the resistance between the voltage differences is increased due to the increase of the surface resistivity. Therefore, there can be less loss in even mode. Even the isolation is not much improved over the frequency range, it is possible to see that insertion loss is decreased (Fig. 4.13).

It is hard to achieve a good structure with the lower surface resistivity and besides that the production of highly resistive surface is hard to manufacture. If we had been able to manufacture it with  $1000 \Omega/\text{sq}$  it would have been a nearly infinite bandwidth power divider/combiner structure. In previous section, it is also shown that splitting the resistance plane would be able to decrease the even mode loss. However, very thin resistances are also hard to manufacture (i.e. 0.1 mm). As the future work, it is possible to redesign both of the dividers for the high precision processes such as the thin film.

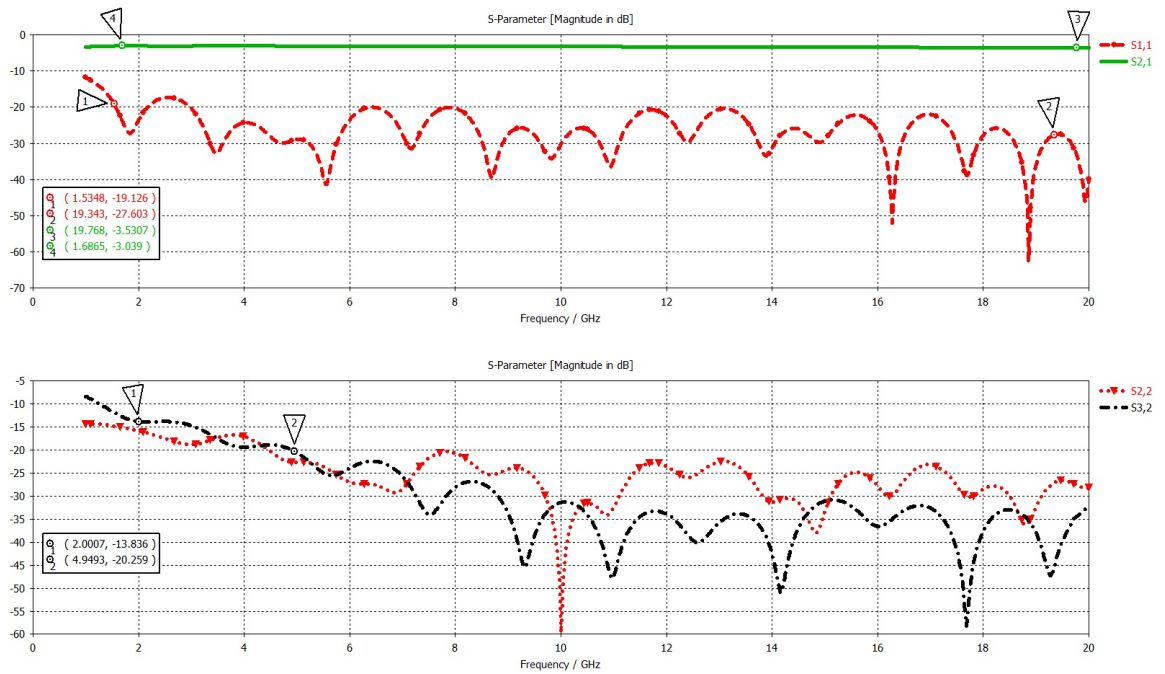


Figure 4.13: EM Simulation of continuous tapered divider with  $1000 \Omega/\text{sq}$  surface resistive material

# Chapter 5

## Conclusion

In this thesis a new power divider/combiner design has been studied based on the Wilkinson power divider/combiner and the tapered lines. The tapered lines are used to improve the frequency response of the even mode. It has been understood that it is possible to achieve an ultra wideband frequency range due to the continuity of the tapered line. Still, the tapered line has the size problem. The Smith chart response of the tapered line exposes that the input matching can be adjusted with a series capacitance for the lower frequencies.

The odd mode structure of the proposed divider/combiner limits the higher frequency of the bandwidth. Four different options have been used to calculate the isolation resistors. These options can easily be used for designing N section Wilkinson power divider/combiner. However, the bandwidth of the Wilkinson divider is limited by its even mode. Without adding any additional element to the isolation resistors, it is possible to achieve a high bandwidth over the isolation. It has been observed that when there is a continuous connection between tapered lines, there are multiple paths that cause insertion loss. In order to fix that problem, a high surface resistivity material has to be used or a continuous resistor has to be discretized. These models have not been manufactured yet, due to the manufacturing difficulties. On the other hand, a proposed model for an eight section power divider/combiner with the discrete chip resistors has been manufactured. The results show that it is possible to design an ultra high bandwidth

power divider/combiner structure with the proposed improved tapered lines that has larger bandwidth than the classical N-section Wilkinson divider.

The proposed structure can be designed with the guideline given in the Figure 5.1.

1. The frequency band of the divider combiner should be determined for -20 dB level for the isolation and input return losses.  $f_2$  is the upper frequency cut-off and  $f_1$  is the lower frequency cut off.
2. The tapered line is used in the even mode structure of the design. Since, the tapered line is a half wavelength structure, a tapered line should be designed for  $2f_1$  frequency.
3. The designed tapered line can be improved with a series capacitance at the input side. Therefore, the lower cut off frequency is extended to the  $f_1$  frequency.
4. The odd mode analysis of the structure limits the upper frequency  $f_2$ . There are four different options to decide the isolation resistor values. Depending on the bandwidth and the power handling capacity, any of the options listed below can be chosen.
  - The linear variation method.
  - The improved linear variation method.
  - The equal power dissipation method.
  - The improved equal power dissipation method.
5. The isolation resistors are constructed with the surface resistive materials (ohmic sheet). The decision of this material is crucial for the design of the isolation resistors and also for the unexpected even mode losses.
6. Due to the parasitics that can not be simulated in the schematic model, the EM simulation can slightly differ from the original design. It is possible to avoid these parasitics by small optimizations of the EM model.

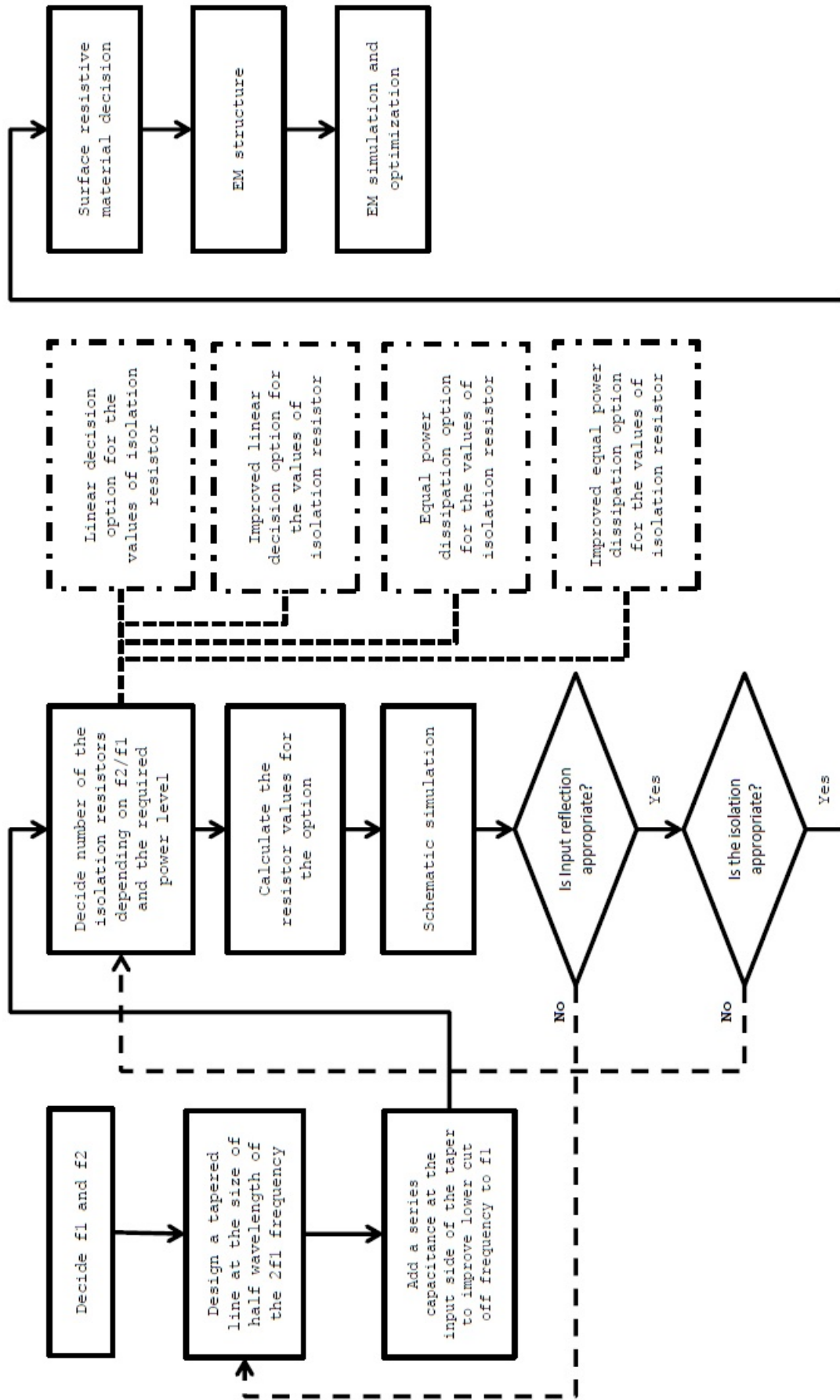


Figure 5.1: Design guideline for the proposed power divider combiner.

# Bibliography

- [1] D. M. Pozar, *Microwave Engineering*. Wiley-IEEE Press, 2011.
- [2] E. Wilkinson, “An n-way power divider,” *IRE Trans. on Microwave Theory and Techniques*, vol. 8, pp. 116 – 118, 1960.
- [3] S. B. Cohn, “A class of broadband three-port tem-mode hybrids,” *IRE Trans. on Microwave Theory and Techniques*, vol. 19, pp. 110 – 116, 1968.
- [4] J. C. Kao, Z. M. Tsai, K. Y. Lin, and H. Wang, “A modified wilkinson power divider with isolation bandwidth improvement,” *IEEE Transactions on Microwave Theory and Techniques*, pp. 2768–2780, 2012.
- [5] X. P. Ou and Q. X. Chu, “A modified two-section uwb wilkinson power divider,” *2008 International Conference on Microwave and Millimeter Wave Technology Proceedings, ICMMT*, pp. 1258–1260, 2008.
- [6] O. Ahmed and A. R. Sebak, “A modified wilkinson power divider/combiner for ultrawideband communications,” *IEEE Antennas and Propagation Society, AP-S International Symposium*, 2009.
- [7] A. Wentzel, V. Sayed, and G. Boeck, “Novel broadband wilkinson power combiner,” *European Microwave Conference*, pp. 212–215, 2008.
- [8] U. H. Gysel, “A new n-way power divider/combiner suitable for high-power applications,” *Microwave Symposium, 1975 IEEE-MTT-S International*, pp. 116 – 118, 1975.
- [9] R. E. Collin, *Foundations for Microwave Engineering*. Wiley-IEEE Press, 2000.

- [10] R. Klopfenstein, “A transmission line taper of improved design,” *Proceedings of the IRE*, vol. 44, pp. 31–35, 1956.
- [11] P. Goodman, “A wideband stripline matched power divider,” *Microwave Symposium, 1968 G-MTT International*, pp. 16 – 20, 1968.
- [12] F. de Ronde, “A multi-octave matched quarterwave microstrip taper,” *Microwave Conference, 1982. 12th European*, pp. 617 – 621, 1982.
- [13] B. Mencia-Oliva, A. M. Pelaez-Prez, P. Almorox-Gonzlez, and J. I. Alonso, “New technique for the design of ultra-broadband power dividers based on tapered lines,” *IEEE MTT-S International Microwave Symposium Digest*, vol. 1, pp. 493–496, 2009.

# Appendix A

## Code

Example MATLAB Code for resistor calculation:

```
function [power R BW] = impLin2(impFac,N)

Z_0=50;
xx=0:(N+1);
Zeven= Z_0.*exp((xx./(N+1)).*log(2));
hold on
    hold off
%%Resistors
% R = sym(1:N);
% for k = 1:numel(R)
%     R(k) = sym(sprintf('R%d', k));
% end
gdb= -20; % mismatch in dB
gam= 10^(gdb/20)/N;
kp= (1+gam)/(1-gam);
kn= (1-gam)/(1+gam);
Zodd(1)=Z_0;
for n=1:N
    if mod(N,2)==0
```



```

    if mod(n,2)==1
        k=kn;
    else
        k=kp;
    end
else
    if mod(n,2)==0
        k=kn;
    else
        k=kp;
    end
end

R(n)=(N+1-n)*Zodd(n);
Zint(n)=R(n)/(N-n);
Zodd(n+1)=Zeven(n+1)^2/Zint(n);
end

R=N*50:(-50):50;
R(1)=R(1)/impFac;
% syms the;

k=1;
for the=0:0.001:pi
% Zi = sym(1:N);
% Zo = sym(1:N);
Zi(N)=Zeven(N+1)*(j*Zeven(N+1)*tan(the))/(Zeven(N+1));
Zo(N)=Zi(N)*R(N)/(Zi(N)+R(N));
for n = 1:(N-1)
    Zi(N-n)=Zeven(N+1-n)*(Zo(N+1-n)+ j*Zeven(N+1-n)*tan(the))/(Zeven(N+1-n)+Zo(N+1-n));
    Zo(N-n)=Zi(N-n)*R(N-n)/(Zi(N-n)+R(N-n));
end
end

```

```

Gam(k)=(Zo(1)-Z_0)/(Zo(1)+Z_0);
t(k)=the;
k=k+1;
end
GdB=20.*log10(abs(Gam));
plot(t,GdB,'LineWidth',2)
ylabel('\Gamma (\theta) (dB)', 'fontsize',13);
xlabel('\theta', 'fontsize',13);
axis([0 pi -80 0])

set(gca,'xTick',0:pi/8:pi);
set(gca,'xTickLabel',{'0 ','p/8','p/4','3p/8','p/2','5p/8','3p/4','7p/8',
    'fontname','symbol',...
    'fontsize',10)
grid
% real(Zo)

% the=pi/2;
% Zo(1)=subs(Zo(1));
% Gam=(Zo(1)-Z_0)/(Zo(1)+Z_0);
% the=0:0.01:pi;
% Gam =subs(Gam);
% plot(the,abs(Gam))
flow=1;
fhigh=0;
bwlimit=-17;
if min(GdB)<bwlimit
    for n=1:length(GdB)
        if(GdB(n)<bwlimit && flow==1)
            flow=0;
            fhigh=1;
            t1=t(n);
        end
    end
end

```

```

        if (GdB(n)>bwlimit && fhigh==1)
            th=t(n);
            break;
        end
    end
    BW=th/tl;
else
    BW=0;
end
Za(N)=inf;
Zb(N)=R(N);
for k=N-1:-1:1
    Za(k)=Zeven(k+1)^2/Zb(k+1);
    Zb(k)=Za(k)*R(k)/(Za(k)+R(k));
end
    pl(1)=Za(1)/(Za(1)+R(1));
    pr(1)=1-pl(1);
for k=2:N-1
    pl(k)=pr(k-1)*Za(k)/(Za(k)+R(k));
    pr(k)=pr(k-1)-pl(k);
end
    pl(N)=pr(N-1);
sum(pl);
power=1/max(pl);

end

```